Sedimentary Geology 379 (2019) 25–45

Contents lists available at ScienceDirect

Sedimentary Geology

journal homepage: www.elsevier.com/locate/sedgeo

# The late Triassic development of playa, gilgai floodplain, and fluvial environments from Upper Silesia, southern Poland

Karol Jewuła [a,*], Michał Matysik [b,c], Mariusz Paszkowski [a], Joachim Szulc [c]

[a] Institute of Geological Sciences, Polish Academy of Sciences, Senacka 1, 31-002 Kraków, Poland
[b] Michał Matysik Geoconsulting, Malachitowa 5/3, 30-798 Kraków, Poland
[c] Institute of Geological Sciences, Jagiellonian University, Gronostajowa 3a, 30-387 Kraków, Poland

A R T I C L E  I N F O

*Article history:*
Received 26 August 2018
Received in revised form 5 November 2018
Accepted 7 November 2018
Available online 10 November 2018

Editor: Dr. J. Knight

*Keywords:*
Gilgai
Playa
Palaeosol
Vertebrate
Norian
Upper Triassic

A B S T R A C T

The numerous discoveries of disintegrated skeletons of large terrestrial vertebrates within several thin levels of the Upper Silesian Keuper initiated broad investigations into the palaeoenvironment and age of the bone-bearing sediments. Despite years of research, the depositional history of the Upper Triassic continental succession and its controlling factors are still poorly recognized. This paper reconstructs the depositional evolution of the Upper Triassic strata in Upper Silesia, Poland, discusses the tectonic and climatic control on deposition, and identifies the sediment provenance. Detailed sedimentological analysis enabled the recognition of three major palaeoenvironments: (1) playa; (2) distal floodplain featured by gilgai micromorphology; (3) fluvial system (sand-dominated meandering, sand- and gravel-dominated braided, and potentially anastomosing river system). The transition from one palaeoenvironment into another reflects climatic changes throughout the late Triassic. The Carnian interval is dominated by gypsum-rich playa mudstones deposited under hot and arid conditions, with only one wet episode recorded as meandering river sandstones (the so-called Carnian Pluvial Event). In contrast, Norian sedimentation was controlled by strong seasonal climatic variations, which is reflected in alternating palaeosol horizons (vertisols and calcisols), thin claystone beds (small water-pond deposits), and conglomerates (rapid flood events). This facies assemblage was formed in a relatively stable floodplain which became the main habitat of numerous vertebrate organisms. The Rhaetian is represented by a gravel-dominated braided river system developed in response to significant climate humidification, with tectonic controls on flow direction. Clast types from Norian and Rhaetian conglomerates revealed that the studied area was fed from the south and south west by the San River and Moesian Massifs. Geochemical analysis of Norian palaeosol horizons suggests mean annual precipitation of ~720 mm/yr in agreement with the palaeoclimatic reconstructions for the area, pointing to seasonal sub-humid to semi-arid climate conditions.



## 1. Introduction

In recent years, numerous vertebrate and invertebrate remains have been found in Upper Triassic continental facies of Upper Silesia (southern Poland), including reptiles, amphibians, fish, bivalves, and mammals (e.g., Dzik et al., 2000; Dzik, 2001; Sulej, 2002; Dzik and Sulej, 2007; Niedźwiedzki and Sulej, 2008; Świło et al., 2014; Lucas, 2015, Skawiński et al., 2017; Antczak and Bodzioch, 2018a, 2018b; Konietzko-Meier et al., 2018; Sulej et al., 2018). These findings are significant in the understanding of animal evolution, especially as the late Triassic marks the dawn of dinosaurs, pterosaurs, and mammals (Benton et al., 2014). However, this understanding requires the bone-bearing deposits to be placed in a well-constrained chronostratigraphic position and a thorough understanding of the broader palaeoenvironmental context.

Most of the research to date has been focused on bone-bearing levels and except for the western part of the Germanic basin (e.g. McKie and Williams, 2009), little is known about the palaeoenvironmental evolution of the late Triassic in Silesia. The stratigraphy was updated by Racki and Szulc (2015), but a detailed sedimentary model for the Upper Triassic succession in Upper Silesia still needs to be produced and until this is resolved, any evolutionary versus ecological hypothesizes for tetrapod successional changes could be considered as premature.

This paper addresses these shortcomings by reconstructing the depositional history of the Upper Triassic continental strata from Upper Silesia in a broader context of climate, tectonism, and material provenance. It is demonstrated how the palaeoenvironment changed with time between a dry playa, monsoon-controlled floodplain (gilgai

* Corresponding author.
*E-mail address:* ndjewula@cyf-kr.edu.pl (K. Jewuła).

https://doi.org/10.1016/j.sedgeo.2018.11.005

relief dominated), and meandering, braided, and anastomosing river systems, and therefore has the potential to test various climatic hypotheses for the late Triassic. Our sedimentological model can be treated as a baseline for further palaeobiological deliberations.

## 2. Geological setting and stratigraphy

In the late Triassic, the Upper Silesia region formed the most south-easterly part of the subtropical continental Germanic Basin (Fig. 1A).

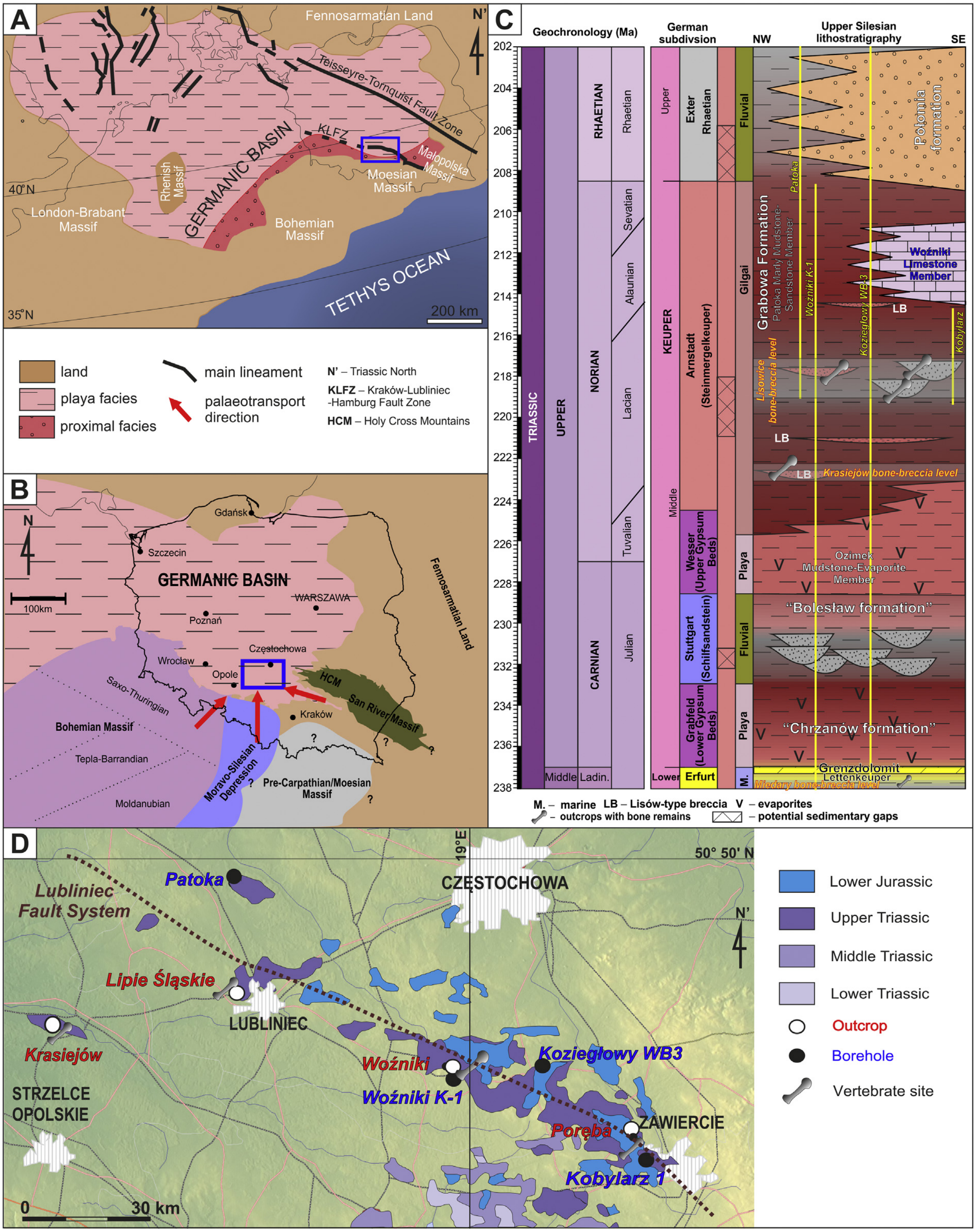


**Fig. 1.** (A) Palaeogeographic map of the Germanic Basin in the Late Triassic. The Upper Silesia region (blue rectangle) was situated in the proximal, SE part of the basin. (B) Location of the studied area (blue rectangle) and potential source areas for Upper Triassic detritus. Outline of the Germanic Basin after Feist-Burkhardt et al. (2008). (C) Geochronological and lithostratigraphic position of the Upper Silesian Keuper Group. Geochronological time scale after International Commission on Stratigraphy (Cohen et al., 2013). German lithostratigraphy after Deutsche Stratigraphische Kommission (Beutler et al., 2005). The extent of potential age gaps after Nitsch (2018). (D) Simplified geological map showing location of the studied outcrops, boreholes, and vertebrate-rich sites, relative to the Lubliniec Fault System (modified from Szulc et al., 2015b). (For interpretation of the references to colour in this figure legend, the reader is referred to the web version of this article.)

The area was bound to the south by the Bohemian, Pre-Carpathian/Moesian, and San River Massifs (Fig. 1B). These lands provided a constant supply of siliciclastic material deposited in fluvial, floodplain, and playa environments. Variegated mudstones and claystones dominate the succession, whereas sandstones and conglomerates are much thinner and geographically limited (Fig. 1C). Rare carbonates formed during short-term marine incursions or in spring-fed pans. Collectively, these sediments are termed as Keuper Group. Most of the vertebrate remains have been found in the Norian Grabowa Formation. Bone-bearing levels have been found in almost all outcrops, but the most known intervals with thousands of bones occur in Krasiejów and Lipie Śląskie (Fig. 1D).

Numerous lithostratigraphic schemes for the Upper Silesian Keuper have been proposed by various authors (for summary see Szulc et al., 2015b), making regional lithostratigraphic correlations difficult. Recently, Szulc and Racki (2015) have established a new formal lithostratigraphy for the Carnian–Norian interval although older units remain informal, i.e., Lower Gypsum Beds ("Chrzanów formation") and Schilfsandstein ("Bolesław formation"). These units (both formal and informal) can be lithostratigraphically correlated with German subdivisions created by the German Stratigraphic Commission (Beutler et al., 2005), although it is widely accepted that sedimentation was diachronous over the Germanic Basin (Franz, 2009) and successively migrated westwards from the Polish to German part of the basin (Szulc, 2000). This migration was linked to the shifting of the Tethyan rift axis from the east to west and/or opening of the Viking Graben (or proto-Atlantic rift system) (Paul et al., 2009).

## 3. Material and methods

### 3.1. Fieldwork

Fieldwork focused on detailed sedimentological logging and was carried out in four Upper Silesian claypits (Fig. 1D). The exposed sections are each <20 m thick (Fig. 2). The outcrop data was supplemented with sedimentological description of four drill cores: Patoka (208 m long), Koziegłowy WB-3 (162 m), Woźniki K-1 (100 m), and Kobylarz also known as Marciszów (54 m). The first three cores penetrated the entire Keuper succession (Figs. 1C; 3–5).

Facies were distinguished based on texture, colour, sedimentary structures, the occurrence of bioturbation structures and faunal and floral remnants. Diagenetic alterations were described where visible. Facies classification is based on modified Miall's (1996) fluvial classification with G, S, M, C, L, D representing dominant grain size/lithotype (gravel, sandstone, mudstone/siltstone, claystone, limestone, and dolomite, respectively). When macroscopic identification of grain size was impossible, the more generic term of mudstone was applied. Grain size is followed by the sedimentary structure type (m – massive/structureless deposit, h –horizontal lamination or bedding, x – low angle cross-bedding or lamination, r – ripple cross-lamination, t – trough cross-bedding, ped – pedogenically modified, evp – evaporitic). Facies are presented in Table 1.

Fluvial components, such as channels, laterally accreted sedimentary bodies, and overbank deposits, were recognized based on the lithofacies association, internal structures, and surfaces bounding individual complexes. Fluvial architecture elements are presented in Table 2.

Palaeosols and their component horizons were identified in cores and outcrops based on macroscopic features, such as colour, pedogenic nodules, slickensides, root structures, and mottles, following the classification of Retallack (2001): (1) dark red, blocky palaeosol without pedogenic concretions – superficial horizon 'A'; (2) angular, blocky structure with clay skins and common mottles – argillic, pedogenic horizon 'B'; and (3) transitional to parent material horizon – horizon 'BC'. The palaeosol horizon modifiers are represented by accumulation of carbonates (k) and presence of slickensides (ss).

### 3.2. Geochemistry

Geochemical ratios were calculated from the geochemical data of Środoń et al. (2014) which were obtained from diagenetic, weathering, and mineralogical study of the Keuper sediments from Upper Silesia. All major elements have been normalized to 100% to take into account loss of ignition (LOI) and then converted from weight percent to molar percent. To characterize and quantify weathering processes, CALMAG (Nordt and Driese, 2010) and CIA-K (Sheldon et al., 2002) weathering ratios and their respective Mean Annual Precipitation (MAP) from regression models have been calculated. Chemical (major, trace, and rare earth elements, REEs) and mineralogical data, and weathering ratio calculations are provided in Supplementary Material 1.

### 3.3. Gravel analysis

Gravel analysis from Patoka-1 well has been performed to quantify compositional groups of the 8–16 mm grain size fraction. Two bulk samples from the deepest coarse-grained intervals of Grabowa and Połomia formations were collected and underwent microscopic identification of the grain types. Among many Norian gravel beds and intercalations within the mudstone carbonate Grabowa Formation, only dispersed clasts above 9 mm have been qualitatively studied. The quantitative results for the Rhaetian Połomia Formation are provided in Table 3.

## 4. Results and interpretation

### 4.1. Depositional facies

Fifteen major Upper Triassic lithofacies were identified. The detailed characteristics and interpretation of each facies and their associations are given in Tables 1, 2, and 4. The facies are dominated by siliciclastics which consist of various proportions of quartz grains and clay minerals. Sediments rich in clay minerals are characterized by a massive structure and were classified as massive claystone (Cm) interpreted as having been formed in ephemeral ponds developed in the localized topographic depressions.

With increasing quartz content, claystone grades into mudstone that is mainly massive (Mm), horizontally-laminated (Mh), or ripple cross-laminated (Mr). The three facies were most likely deposited in distal overbanks during flood events, with the first two facies representing tranquil low-flows to stagnating waters and the latter facies being accumulated by high-energy flows. Locally, some mudstones are pedogenically altered (Mped), or rich in evaporite nodules and veins (Mevp).

Fine- to coarse-grained sandstones with a massive structure (Sm) or low-angle cross-stratification (Sx), horizontal lamination (Sh), ripple cross-lamination (Sr), trough cross-stratification (St), pebbly sandstones (Sg), and clast-supported (Gcs) and matrix-supported (Gms) conglomerates are all associated with fluvial environments. Sandstones generally formed as channel-fills, bars, and crevasse splays, while conglomerates are considered as high-density flow deposits related to catastrophic runoffs.

Minor carbonates (D, L) are either of marine (Grenzdolomit), palustrine or hydrothermal origin (Woźniki Limestone Member). These facies were described elsewhere (e.g., Szulc et al., 2006).

### 4.2. Small-scale vertical and horizontal arrangement of depositional facies

The distinguished facies display no cyclic organization in a vertical profile and instead are arranged in various configurations and random alternations (Figs. 1–4). The contacts between successive facies are generally sharp and are conformable where a fine-grained sediment overlies a coarse-grained deposit or are erosional where a reversed

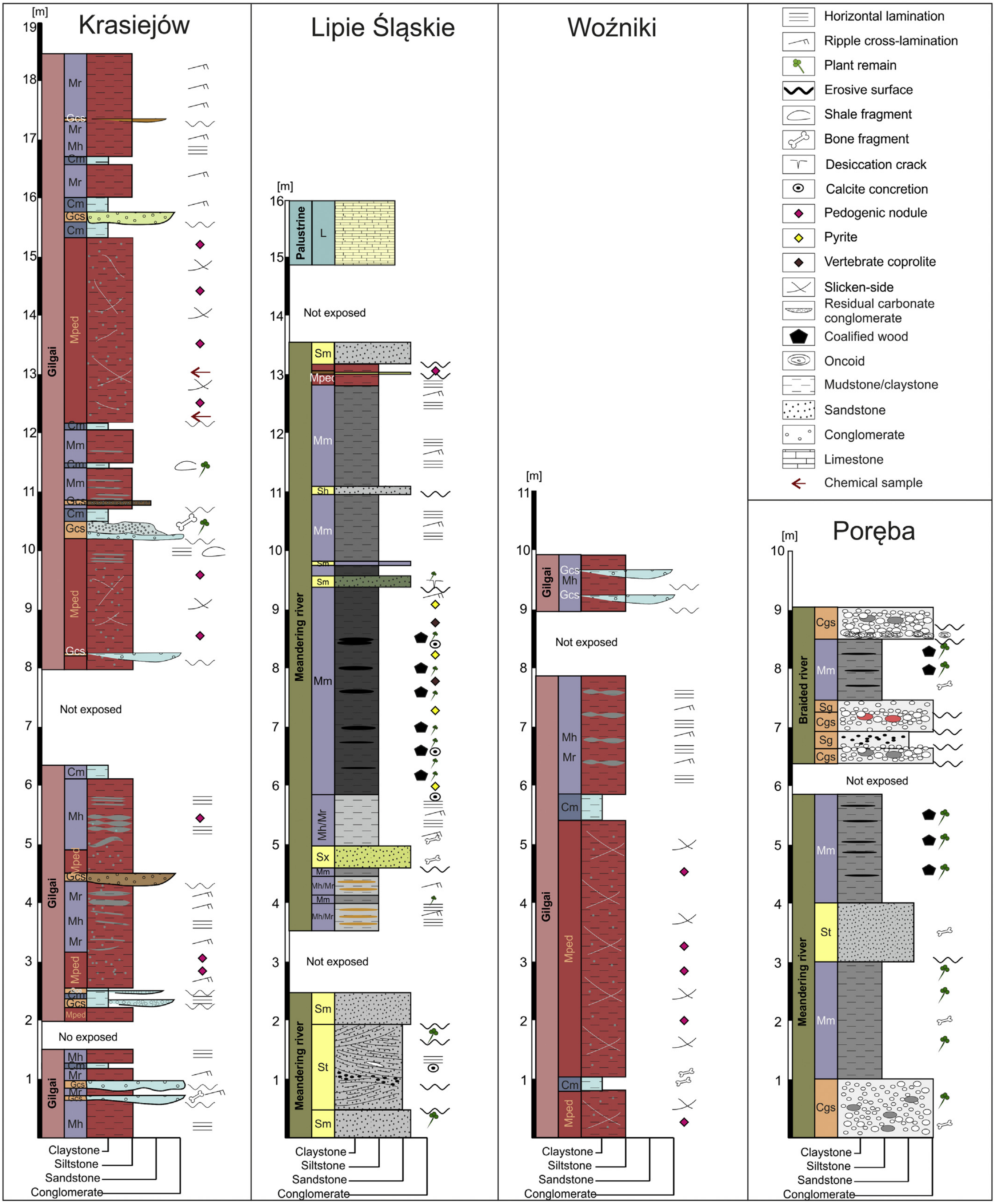


**Fig. 2.** Sedimentological logs for Krasiejow, Lipie Śląskie, Woźniki, and Zawiercie outcrops, representing various intervals of the Norian Patoka Member (Grabowa Formation). Note large-scale vertical changes in sediment colour and composition, interpreted to reflect climatic changes in the area. The Woźniki log is modified and reinterpreted from Szulc et al. (2015a). For facies codes see Table 1. (For interpretation of the references to colour in this figure legend, the reader is referred to the web version of this article.)

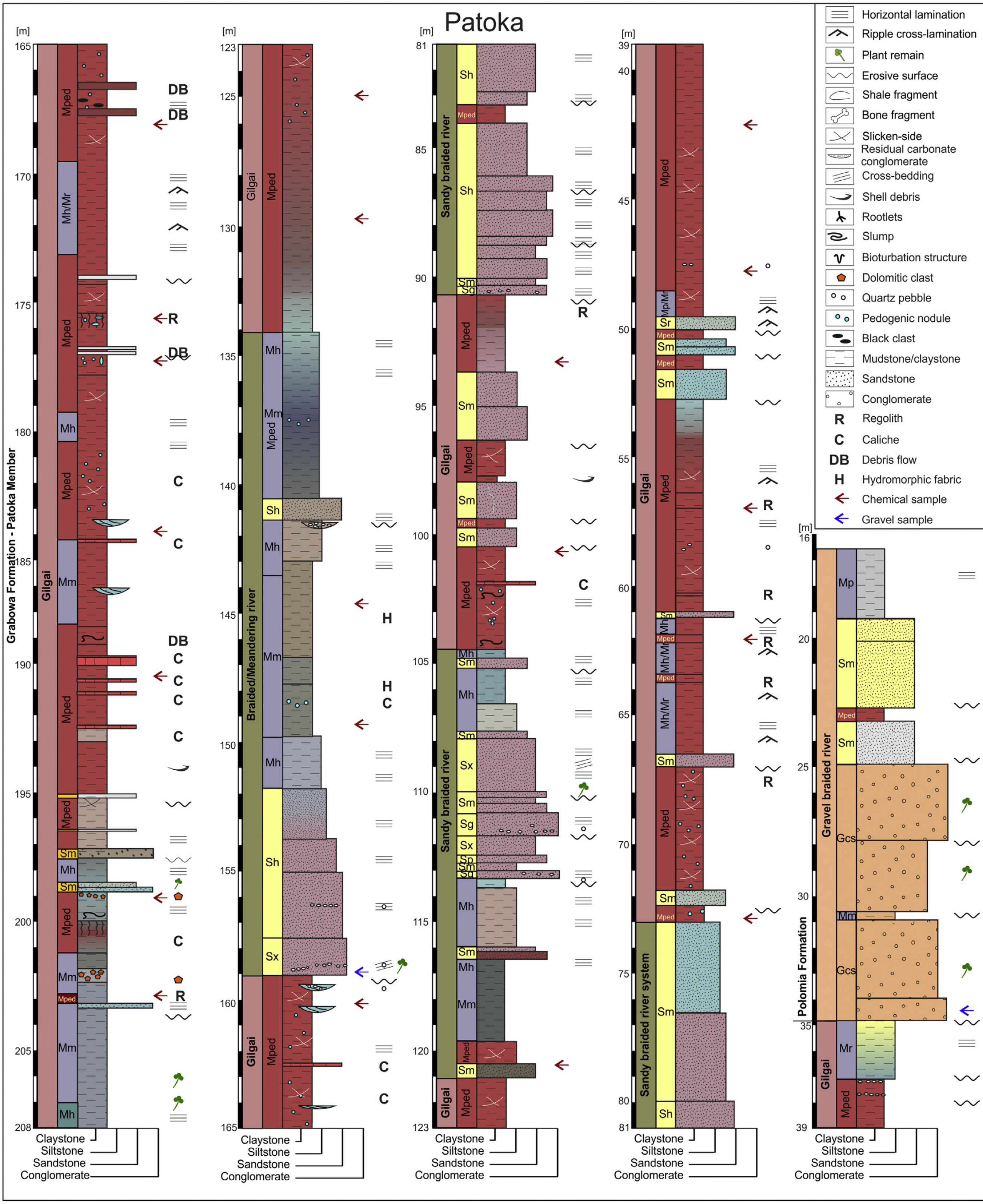


**Fig. 3.** Sedimentological log for Patoka well penetrating the upper half of the Norian Patoka Member (Grabowa Formation) and the entire Rhaetian. For facies codes see Table 1.

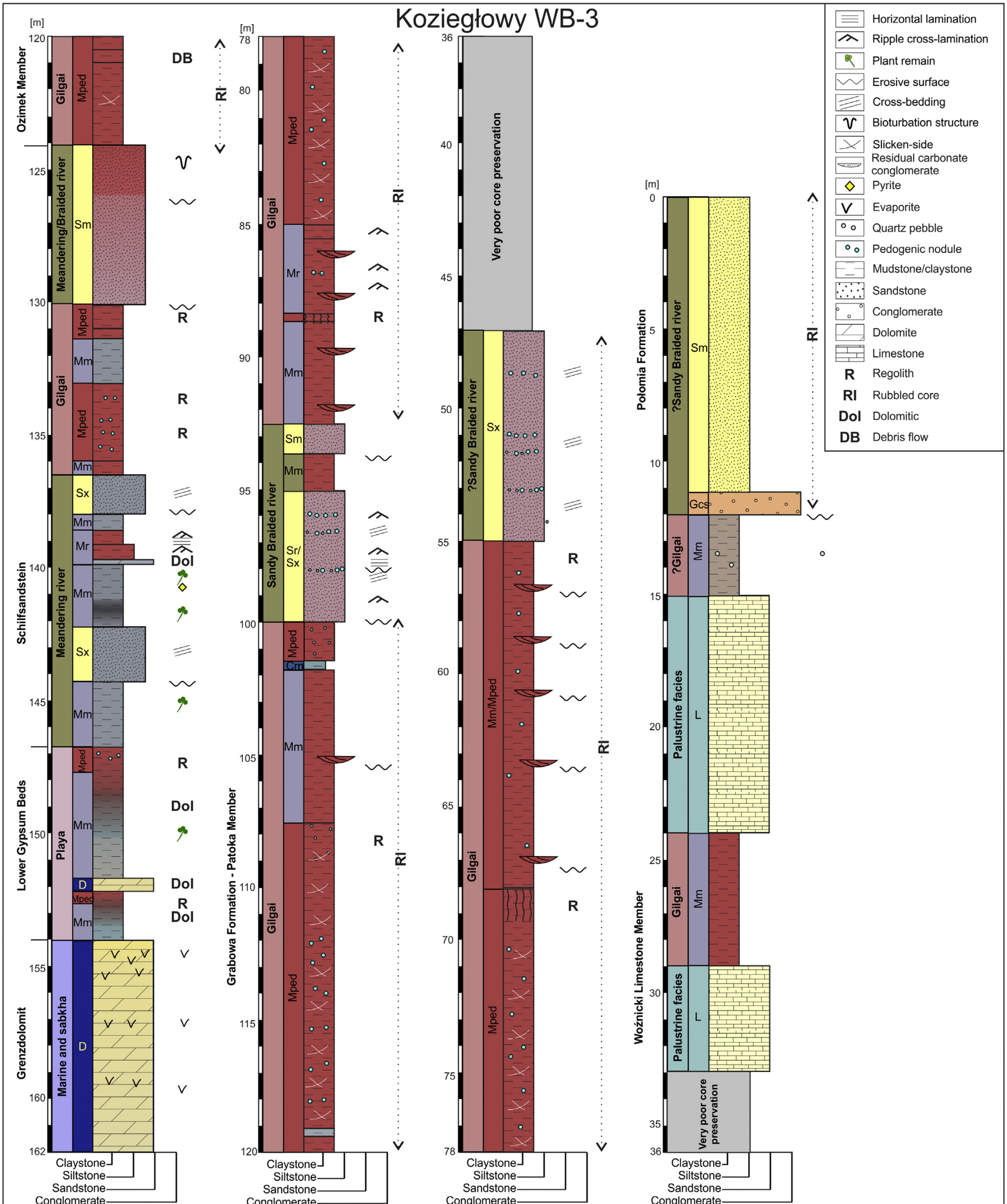


**Fig. 4.** Sedimentological log for Koziegłowy WB-3 well penetrating the entire Upper Silesian Keuper, from the Ladinian Grenzdolomit to the Rhaetian Połomia Formation. For facies codes see Table 1.

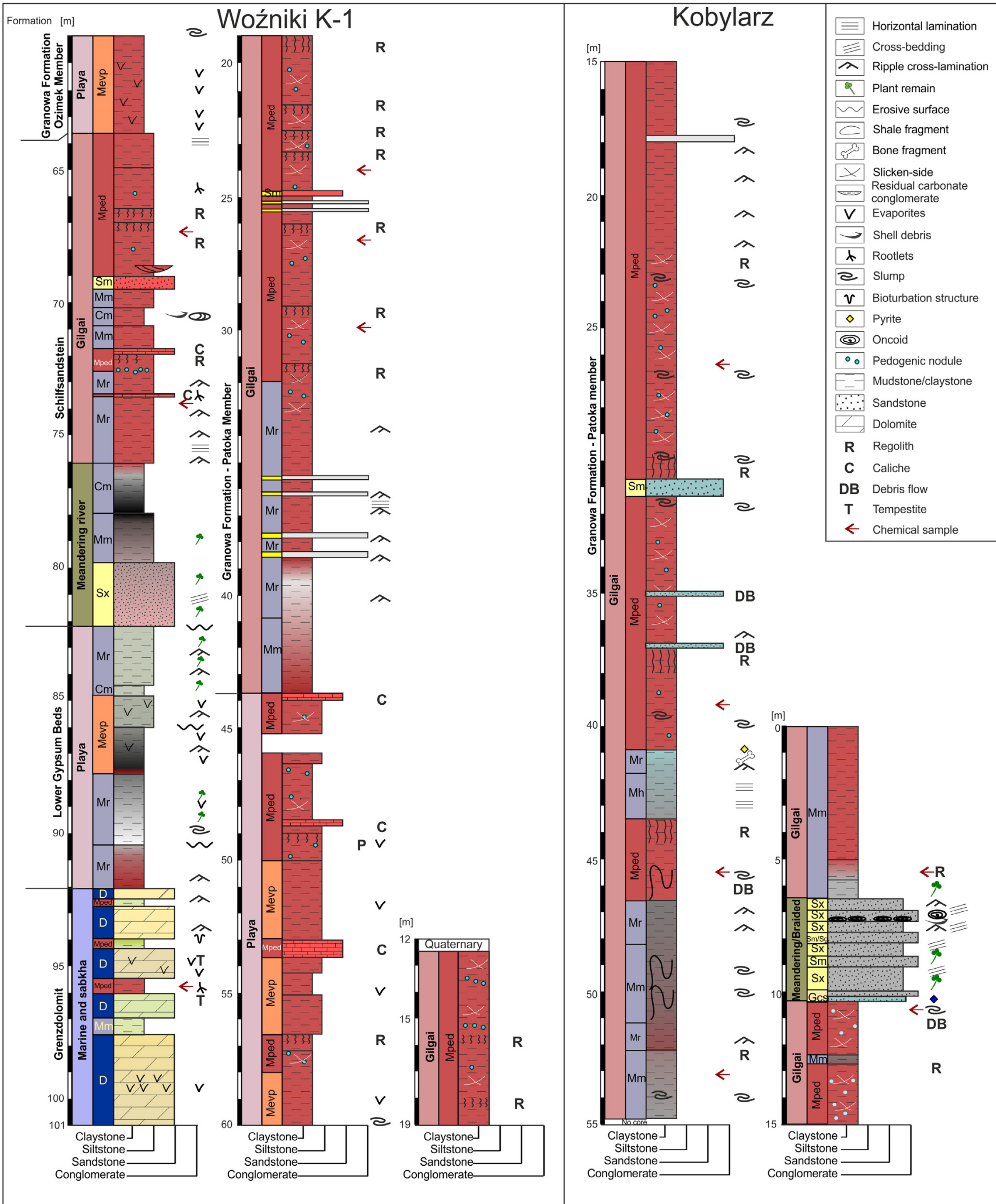


**Fig. 5.** Sedimentological logs for Woźniki K-1 (Ladinian-Rhaetian) and Kobylarz (Norian) wells. For facies codes see Table 1.

facies succession occurs. In the latter case, the depth of erosion is unknown. Locally, a gradual fining-upward transition from conglomerate, through sandstone, to fine-grained facies is observed.

Claystones (C) and mudstones (M) dominate volumetrically and are laterally persistent at the outcrop scale, and perhaps could be correlated between neighboring localities if any marker beds or biostratigraphic

**Table 1**
Description and interpretation of depositional facies in the Upper Triassic of Upper Silesia.

| Facies | Description | Depositional process and setting |
|---|---|---|
| Massive claystone (Cm) | White and beige, structureless, locally silty, calcareous claystone forming up to 20 cm thick and dm to m-wide, irregularly shaped lenses. Lower and upper boundary commonly sharp. Local rare bivalves (e.g., *Unio* sp.) (Fig. 6A–B). | Deposition by suspension fallout within ephemeral shallow ponds developed in local depressions. |
| Massive mudstone (Mm) | Variegated and grey, structureless, friable mudstone with blocky cleavage. Gradual or sharp base. Occasional faint planar or ripple-cross lamination, white calcareous nodules, and/or carbonaceous matter. Locally disturbed. Thickness from several centimeters to 5 m (Fig. 6A–B). | Dark grey, grey and beige mudstone with floral remains – infill of small local basins, possibly oxbows or waterholes. Variegated mudstone with calcareous nodules and/or sharp bases – high-density mud flow deposit (Szulc, 2005). |
| Pedogenically modified mudstone (Mped) | Dark red, red, bluish, and grey, friable, blocky mudstone with predominant mottled texture. Local root structures and slickensides. Base sharp or gradual, top irregular often overlaid by planar or ripple cross laminated mudstones Thickness from a few millimeters to 4 m (Fig. 6C–E). | Primitive soil (inceptisol/regolith) and palaeosol (vertisol and calcisol) developed on floodplains. |
| Evaporitic mudstone (Mevp) | Dark red, red, and variegated mudstone with gypsum aggregates (up to 10 cm across) and veins (up 2 cm thick). Common thin caliche intervals (Fig. 6F). | Distal floodplain with transpiration exceeding precipitation to promote gypsum crystallization. |
| Horizontally laminated mudstone (Mh) | Variegated mudstone with distinct mm-scale horizontal lamination. Local *Skolithos* isp. and undetermined burrow mottles (Fig. 6G–H, K) | Deposition by tranquil low-flow or from suspension (Simon and Gibling, 2017b). *Skolithos* burrows indicate relatively firm substrate. |
| Ripple cross-laminated mudstone (Mr) | Variegated mudstone with mm- to cm-scale sets of ripple cross lamination, commonly truncated and/or with sub-critical climbing. Abundant silty streaks and interlaminae (Fig. 6G–I) | Flood-type deposit formed under variable energy flow: transition from ripple cross-lamination to planar lamination represents gradual decrease in the fluid flow velocity, while climbing-ripple cross-lamination is associated with very high rate of suspension fall-out relative to the rate of ripple migration (Collinson et al., 2006). |
| Massive fine-grained sandstone (Sm) | Beige and grey, well-cemented, structureless sandstone with well-sorted quartz grains ranging in size from mid fine to upper fine. Common normal grading. Local carbonaceous matter and quartz pebbles. Thickness 1 to 3 m (Fig. 7A). | Rapid deposition from highly concentrated, heavy leaden (hyperconcentrated) laminar sediment/water flows in ephemeral rivers (Horn et al., 2018). |
| Trough cross-stratified sandstone (St) | Beige, grey, and dark grey, well-sorted, fine- and medium-grained sandstone organized into dm-scale cross-bedded trough sets, stacked to form up to 3 m thick units. Individual sandstone troughs typically display lenticular shapes. Small-scale sedimentary structures represented by planar or very low angle (up to 5°) laminae and cm-scale oscillatory or climbing-ripple cross laminae. Common carbonaceous detritus and pyrite nodules. Local strong calcite cementation. Occasional convolute structures. | Trough cross-bedding can be attributed to migration of lower flow regime 3D dunes (Collinson et al., 2006), commonly linguoid in form. In-channel position. |
| Low-angle cross-stratified sandstone (Sx) | Beige, grey, and dark grey, fine-grained and rarely medium-grained sandstone, moderately to well sorted, showing low-angle (up to 20°) lamination or bedding. Lamination picked out by grain-size variation or dispersed plant debris. Individual sets thickness varies from a few cm to m. Laminasets tops and bottoms are erosive. Laminasets are organized in cosets up to 2 m thick (Fig. 7C–D). | Aggradation and migration of small to medium size 2D microforms (such as straight-crescent dunes) deposited in the transition between subcritical and supercritical flows. |
| Ripple cross-laminated sandstone (Sr) | Beige, grey, and dark grey, well-sorted, weakly cemented, fine to medium grained sandstone with climbing current ripple cross-lamination. Thickness from a few decimeters to 3 m (Fig. 7E). | Thicker units deposited under lower bed condition within point-bars on the channel margins; thinner units sandwiched between mudstones can be attributed to crevasse splays. Deposition and reworking by turbulent sub-critical flows that generated 2D/3D dunes (Ielpi and Ghinassi, 2015). |
| Horizontally laminated/bedded sandstone (Sh) | Beige, grey, and dark grey, well-sorted, fine- and medium-grained sandstone with mm-scale horizontal lamination and locally bedding. Common dispersed plant remains. Thickness between a few decimeters to 3 m (Fig. 7A–C, F). | Flood or high-flow deposit within the channel belt or, crevasse splays if thickness is relatively small (<1 m) and the sediment is embedded within the mudstone interval. Deposition and reworking by perennial, turbulent-subcritical flows that generated bedload sheets (Ielpi and Ghinassi, 2015). |
| Pebbly sandstone (Sg) | Beige and grey, medium- and coarse-grained, poorly-sorted sandstone with parallel lamination and quartz and mudstone flat pebbles up to 5 cm long (Fig. 7H–J). | Deposition within fluvial channels of heavy-loaded fluvial system. Mudclasts suggests reworking of old lag deposits (Ielpi and Ghinassi, 2014). |
| Matrix-supported conglomerate (Gms) | White, grey, and light grey, poorly sorted conglomerate with loosely organized oncoids and subangular to subrounded clasts of claystone, quartz, dolostone, limestone, and/or pedogenic sediment. Clasts oriented chaotically or parallel to bedding planes, rarely imbricated. Matrix composed of moderately to poorly sorted, fine- and medium-grained sand (Fig. 7H–J). Occurs astabular or lenticular sedimentary bodies rarely exceeding 50 cm in thickness. | Deposition from high-density bedloads and suspended load flows, related to ephemeral unconfined sheet-floods or braided fluvial/alluvial fan systems. |
| Clast-supported conglomerate (Gcs) | White, grey, and beige, well-cemented conglomerate with densely packed, angular claystone clasts, subrounded to well-rounded granules of pedogenic nodules, and subordinate quartz pebbles. Bed bases sharp and undulating with common load marks. Bed tops either sharp or fining upward into sandstone or siltstone. Individual beds up to a few cm thick and commonly organized in a few-meters wide sheets (Fig. 7G, J). | Deposition by high-density flows. The lateral extent of these conglomerates suggests high-density floods causing redeposition of pedogenic nodules in unconfined or poorly confined conditions. |
| Limestone (L), dolostone (Dol) | This wider group includes nodular limestone, oncolite and stromatolite (for their detailed description see Szulc et al., 2006). Limestones form localized bodies up to 30 m thick. Some limestones show secondary dolomitization features. | Pedogenic, swamp, and spring deposits, partly of hydrothermal origin (Szulc et al., 2006). |

control existed. In contrast, sandstones (S) and conglomerates (G) form m- to dm-wide lenses that cannot be traced from one site to another.

### 4.3. Facies associations

Three major facies associations can be distinguished for the Carnian–Rhaetian interval, based on the vertical and lateral distribution of the lithofacies and their internal architecture: floodplain, playa, and fluvial depositional settings. For summary see Table 4.

#### 4.3.1. Floodplain facies association

*4.3.1.1. Description.* The floodplain environment is dominated by overbank fines: red or variegated mudstones and claystones that are massive (Cm, Mm), horizontally laminated (Mh) or ripple cross-laminated (Mr), up to 2 m thick with marked lateral variation in thickness. Lamination is visible mainly due to subtle changes in the grain size or dispersed plant detritus concentrated on inclined lamina surfaces. Ripple cross-laminated sets show sharp bounding surfaces, abundant

**Table 2**
Fluvial Strata Architecture.

| Architecture element | Lithology, grain size, geometry, and dominant lithofacies | Interpretation |
|---|---|---|
| Gravel bars and bedforms (GB) | Matrix- and clast-supported conglomerates with angular or subangular clasts, medium to coarse-grained sandstones, commonly organized in lenticular or sheet geometry. Main lithofacies: Gms, Gcs, St, Sr, Sh, Sx, | Sheet flood deposits and channel fills of the braided river system. |
| Sandy bedforms (SB) | Fine- to coarse-grained sandstones organized in lenticular, wedge or sheet-like units with clear base erosional surfaces. Main lithofacies: Sh, St, Sr, Sm, Sx, | Channel fill point bar, and crevasse splay deposits. |
| Laminated sandstone sheets (LS) | Fine- and medium-grained sandstones organized in sheet-like units with erosive bases. Main lithofacies: Sh, Sr, Mh, Mm. | Sheet flood and crevasse splay deposits. |
| Overbank fines (OF) | Laterally extensive claystones, mudstones, siltstones, and fine-grained sandstones. Main lithofacies: Cm, Mr, Mped, Mh. | Overbank and flood deposits (gilgai). |

**Table 3**
Main type of clast percentage composition: P-2- sample of 8–16 mm fraction from the Połomia gravel ($n = 120$); averaged interval 26.5–28 m from Patoka 1 borehole.

| Clast lithology | Percentage in sample from Połomia Formation |
|---|---|
| Quartzite: quartz arenite metaquartzite etc. | 16 |
| Jaspilite | 4 |
| Chert fossiliferous, silicified limestone, ganister (silcrete) | 16 |
| Vein quartz | 54 |
| Metachert | 5 |
| Meta-siltstone | 2 |
| Carbonate: Woźniki limestone, coated grain from Lisów breccia, etc. | 3 |

climbing features, and various palaeotransport directions (Fig. 6H), with the dip angle of individual laminae rarely exceeding 20°.

Palaeosols and regoliths (Mped) are also common in this environment and vary in thickness from a few centimeters to 4 m, showing lateral thickness changes (Fig. 6C–E). They form friable, angular to sub-angular, dark red to red, moderately to highly-calcareous, silty intervals with scattered mm- to cm-scale (up to 4 cm in diameter) subrounded to rounded, light grey calcareous nodules, locally forming thin (up to 20 cm thick) irregular layers (Fig. 6D). Palaeosols additionally comprise mm-scale bluish-greyish mottles with distinct boundaries and clay-skinned, concave slickensides having complementary sets of planes with dip angles up to 45°. Greyish-bluish gleying hydromorphic features, small root canals (up to 20 cm long) with diffusive boundaries (rhizohaloes), and/or massive, rarely fibrous, white hardpan-type calcretes up to 50 cm thick are locally present (Fig. 8E).

Fine-grained sediments are intercalated with well-sorted, massive sandstones (Sm), matrix-supported calcareous conglomerates (Gms) or fining-upward, clast-supported conglomerates (Gcs; Fig. 6B, G), occurring as m-scale and cm-thick lenses or layers (Fig. 6B). Locally, bone-bearing levels with numerous cm-long bone fragments and undetermined cm-scale straight or slightly concaved burrows filled with red or grey silty material can be seen (Fig. 6J–K). Rare carbonate intervals comprise white or yellowish micritic limestones interbedded with grey or red, friable marls.

*4.3.1.2. Interpretation.* This facies association is interpreted to have been formed in a distal, mud-dominated floodplain, occasionally affected by catastrophic flashfloods. Mudstones with horizontal and ripple cross-lamination (Mh and Mr) were deposited under vigorous water flows and represent migration of small-scale bedforms in lower and upper flow conditions, likely related to the final stages of floods (Reineck and Singh, 1980). The mottled structure of claystones and mudstones most likely reflects seasonal changes in the groundwater table, which are frequently accompanied by local variations in redox conditions (Mücke, 1994). The scarce and undiversified trace fossils are dominated by shallow burrows of feeders and aquatic dwellers that colonized top parts of the sheet deposits, controlled by local hydrodynamic conditions (Sarkar and Chaudhuri, 1992). Alternatively, laminated mudstones may represent a channel infill with significant vertical aggradation in an anastomosing-type low-energy river system (Gruszka and Zieliński, 2008).

Palaeosols developed within abandoned flood-event deposits during relatively calm periods. Conglomerates composed of calcareous pedogenic nodules (locally known as the "Lisów breccia" which even became an informal lithostratigraphic unit), suggest localized recycling of the soil intervals, winnowing of fine material, and further transport as a clast-supported debris flow during catastrophic run-offs (Szulc, 2005;

**Table 4**
Facies associations and their stratigraphic architecture. Lithofacies abbreviations are consistent with Table 1.

| Lithostratigraphic unit | Facies association | Lithofacies | Architectural elements | Interpretation and depositional environment |
|---|---|---|---|---|
| Rhaetian (Połomia formation) | Braided fluvial system. | Gcs, Sx, St, Sr? | Gravel bars and bedforms (GB), and sandy bedforms (SB). | Gravel- and sand-dominated braided fluvial system. |
| Grabowa Formation (Woźniki Limestone Member) | Floodplain mudstones with freshwater carbonates, rarely multi-storey braided river. | Gcs, Sx, St, Sr, Sg, Mh, Mped, L | Overbank fines (OF) and sandy bedforms (SB). | Mud-dominated distal floodplains with freshwater carbonates developed along fault zone. Localized sand-dominated braided |
| Grabowa Formation (Patoka Member) | Meandering Fluvial System | Sx, St, Sr, Sm, Sh, Mr., Mped, | Overbank fines (OF) and sandy bedforms (SB). | Meandering river system with overbank oxbow deposits. |
| Grabowa Formation (Patoka Member) | Braided Fluvial System | Gms, Sg, Sm, Sr, Sh, | Gravel bars and bedforms (GB), sandy bedforms (SB), and overbank fines (OF). | Sand-dominated braided system developed along the uplifted blocks? |
| Grabowa Formation (Patoka Member) | Floodplain System | Gcs, (Sr), (Sh), Mr., Mh, Mped, Cm | Overbank fines (OF), sandy bedforms (SB) and laminated sandy sheets (LS). | Mud-dominated distal floodplains with sheet-flood deposits, silt-dominated anastomosing river system. and palaeosols (Gilgai). |
| Grabowa Formation (Ozimek Member) | Playa System | Mm, Mped, Mh, Mevp, Sh, | Overbank fines (OF) and laminated sandy sheets (LS)? | Evaporitic deposition in mudflat-playa environments with periodic palaeosol formation. |
| "Bolesław formation" (informal unit) Schilfsandstein | Meandering Fluvial System | Sx, St, Sr, Sm, Sh, Mr., Mped, | Sandy bedforms (SB), laminated sandy sheets (LS) and overbank fines (OF)? | Meandering river system with overbank oxbow deposits |
| "Chrzanów formation" (informal unit) (Lower Gypsum Beds) | Playa System | Mm, Mped, Mh, Mevp, Sh. | Overbank fines (OF) and laminated sandy sheets (LS)? | Evaporitic deposition in mudflat-playa environments |

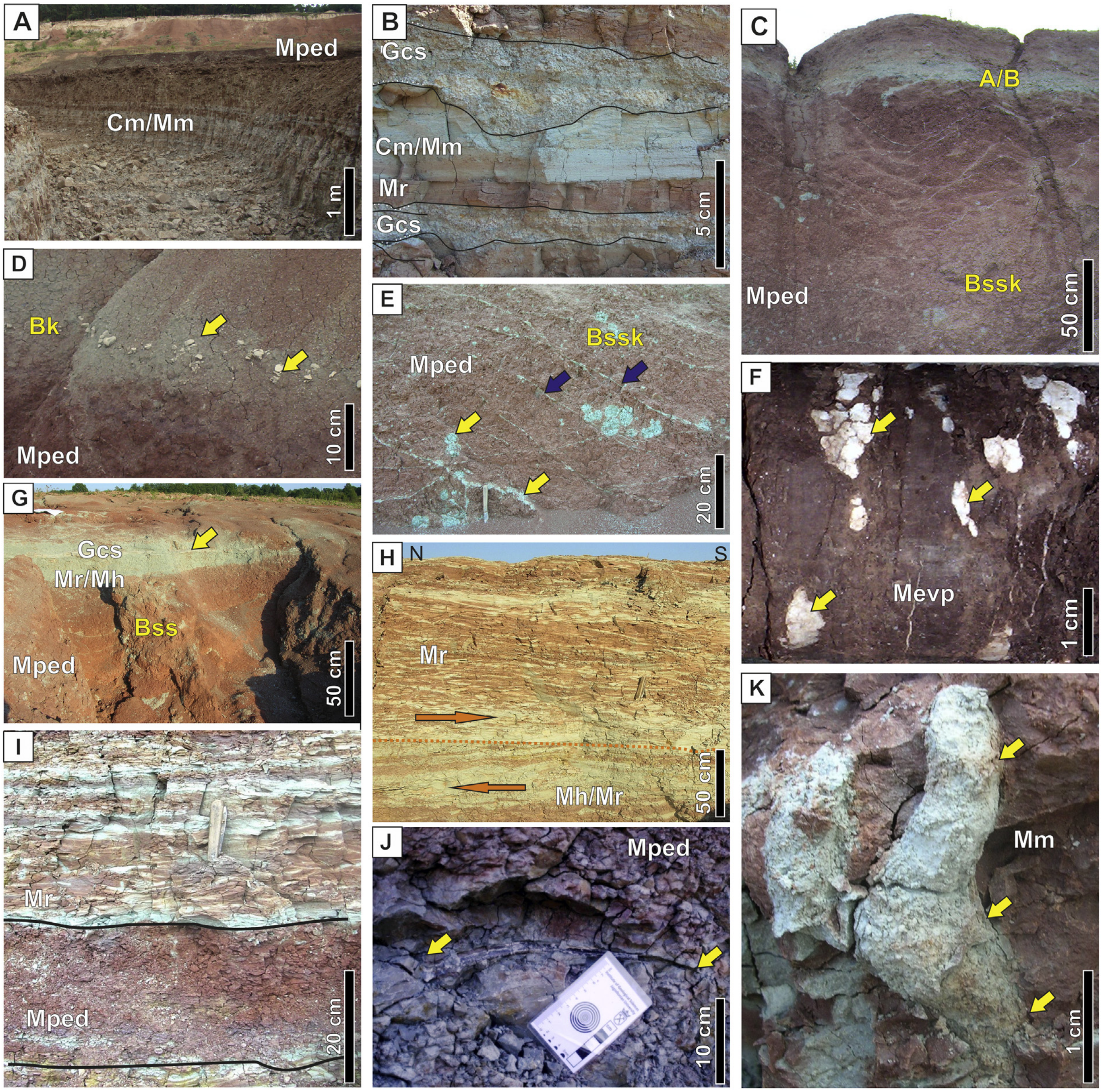


**Fig. 6.** Summary of the claystone and mudstone facies in the uppermost Carnian–Norian Grabowa Formation. (A) Alternation of pedogenically altered mudstones (Mped) and claystones (Cm/Mm). Patoka Member, Patoka clay-pit. (B) Ripple-cross laminated mudstones (Mr) and massive claystones (Cm), interbedded with clast-supported conglomerates (Gcs) composed of reworked pedogenic carbonate nodules and representing flash floods. Patoka Member, Krasiejów. (C) Vertisol profile with well-preserved A and B horizons with slickensides and carbonate nodules (Bss and Bssk horizons). Patoka Member, Krasiejów. (D) Pedogenic carbonate nodules (arrows) in Bk horizon. Patoka Member, Krasiejów. (E) Vertisol with slickenside structures (blue arrows; Bssk horizon) and reductive spots developed around small pedogenic calcareous concretions (yellow arrows). Patoka Member, Krasiejów. (F) Gypsum nodules (arrows) in playa claystone of the Upper Gypsum beds, Ozimek Member, Woźniki K-1 well. (G) Approximately 1-m-thick vertisol horizon. Yellow arrow points at thin conglomeratic beds (flood deposits) and horizontal and ripple-cross laminated mudstones (Mh/Mr). Patoka Member, Krasiejów. (H) Horizontal (Mh) and ripple cross-laminated (Mr) mudstones with different palaeoflow directions (arrows). Patoka Member, Krasiejów. (I) Palaeosol and regolith horizon (Mped) developed on and capped by horizontally laminated floodplain mudstone (Mh). Patoka Member, Krasiejów. (J) Bone fragment (between yellow arrows) in claystone/mudstone, an example of the bone-bearing levels. Patoka Member, Krasiejów. (K) Undetermined shallow burrows (arrows) penetrating reddish massive mudstone (Mm). Patoka Member, Krasiejów. (For interpretation of the references to colour in this figure legend, the reader is referred to the web version of this article.)

Bodzioch and Kowal-Linka, 2012). Isolated carbonate bodies are considered as spring-fed palustrine facies (Szulc et al., 2006).

### 4.3.2. Playa facies association

*4.3.2.1. Description.* Facies assigned to the playa include red marly claystones that are massive (Mm) or locally horizontally laminated (Mh). Evapotranspiration resulted in cm-thick white or greyish amorphic or locally fibrous calcretes, subrounded to rounded calcite nodules up to 2 cm in diameter or irregular gypsum crystal aggregates (Mevp; Fig. 6F). Less abundant are pedogenic intervals (Mped) represented by red friable, highly calcareous mudstones with numerous mm-scale subrounded carbonate nodules, displacive gypsum and/or brecciated fabrics. The pedogenic horizons are up to 3 m thick. Locally, thin fine-grained, well-sorted, horizontally laminated, light red or rarely greenish sandstone intercalations (Sh) are observed. This facies association was recognized only in Woźniki K-1 and Koziegłowy WB-3 wells therefore its lateral extent is unknown.

*4.3.2.2. Interpretation.* The facies association is interpreted to have formed as terminal splays or peneplained continental, saline mudflats (continental sabkhas), under arid and semi-arid conditions when evaporation exceeded precipitation (Simon and Gibling, 2017a). Gypsum nodules likely developed in the ca. 1 m thick capillary zone above the water table (Gunatilaka and Mwango, 1987). Thin, poorly developed soils with calcium and gypsum agglomerates most likely represent aridsols group, specifically calsisols, calgypsols, and gypsols indicative of arid and semi-arid environments (Retallack, 2001). Thin laminated sandstones could have been deposited by episodic floods (North and Davidson, 2012) triggered by torrential rains.

#### 4.3.3. Fluvial facies association

*4.3.3.1. Description.* The fluvial facies association essentially comprises sand- and gravel- dominated facies, whereas fine-grained clastics form only thin intercalations. Sand-dominated facies are represented mostly by fine- and medium-grained sandstones with a massive structure (Sm), trough cross-bedding (St) or large scale cross-bedding (Sx) or smaller-scale sedimentary structures, such as ripple cross-lamination (Sr) and horizontal lamination (Sh), (Fig. 7A–E). The coarser-fraction intervals are frequently overlain by low-angle cross-bedded sandstone-mudstone heteroliths showing a down-dip thickening of sandstone sets (Sx) and an up-dip increasing contribution of siltstone interbeds with ripple cross-lamination (Mr). The heteroliths are laterally or vertically juxtaposed to dark grey and black, massive or horizontally laminated mudstone rich in a pyritized organic matter (both faunal and

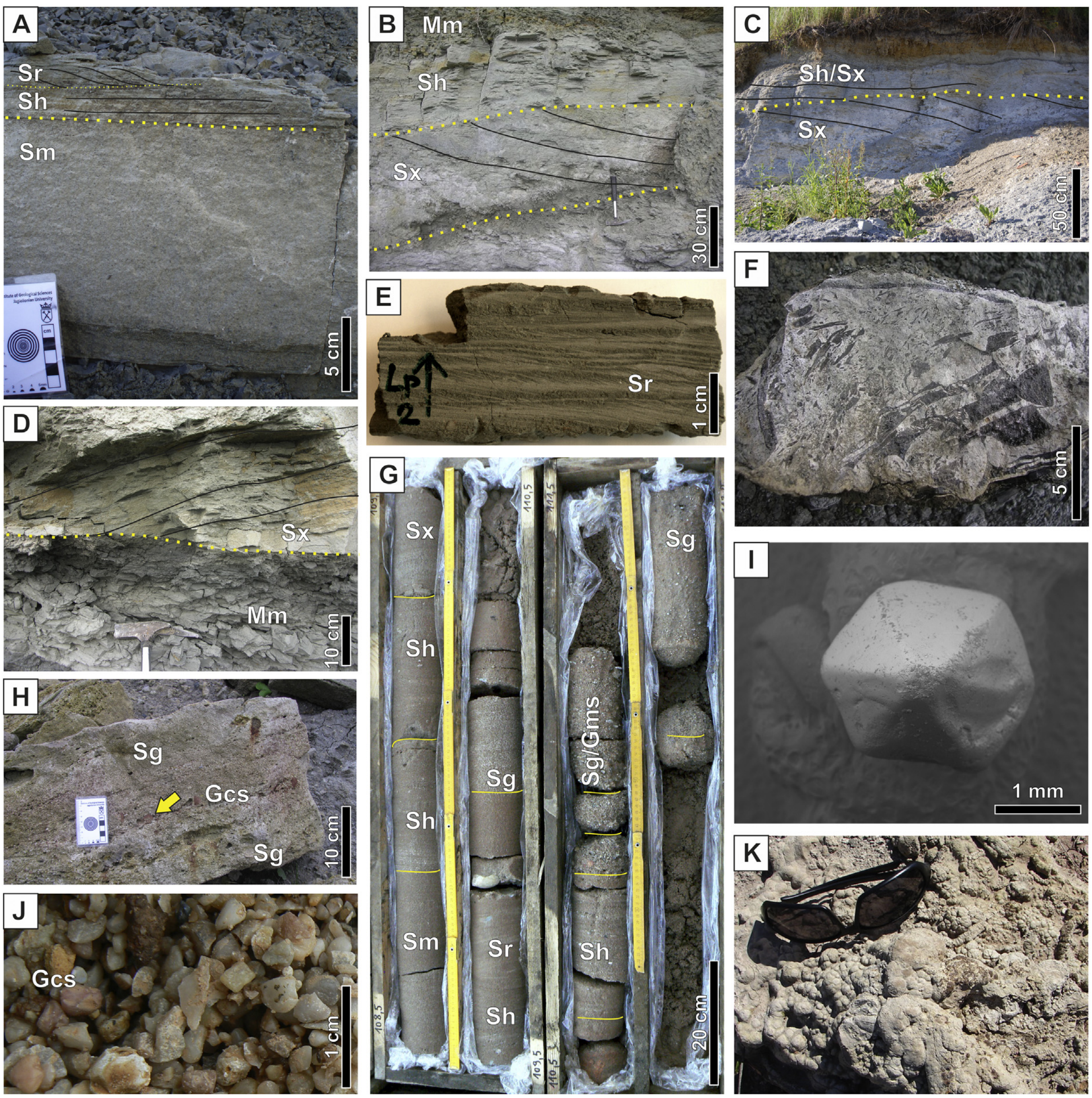


**Fig. 7.** Summary of the sandstone and conglomerate facies in the Upper Silesian Keuper. (A) 'Bouma-like' sequence with massive sandstone (Sm), horizontally laminated sandstone (Sh), and ripple cross-laminated sandstone (Sr), reflecting gradual decrease in the flow discharge in fluvial channel facies. Patoka Member, Lipie Śląskie. (B) Low angle tabular low angle cross-bedded sandstone (Sx) capped by horizontally-bedded sandstone (Sh) and younger massive dark mudstone (Mm). Erosive surfaces are marked by yellow dashed lines. Patoka Member, Lipie Śląskie. (C) Large-scale cross-bedded sandstones (Sx, Sh). Patoka Member, Lipie Śląskie. (D) Cross-bedded sandstone (Sx; lateral accretion of bar) truncating organic-rich mudstone (Mh/Mm; oxbow deposit). Patoka Member, Lipie Śląskie. (E) Ripple cross-laminated sandstone (Sr). Patoka Member, Lipie Śląskie. (F) Massive sandstone (Sm) with well-preserved wooden charcoaled fragments (black components). Patoka Member, Lipie Śląskie. (G) Matrix-supported conglomerate, pebbly sandstones, and cross- and horizontally laminated sandstones (Gms, Sg, Sx, and Sh) with erosive boundaries (yellow lines). Sand-dominated braided river channel facies (Patoka Member, Patoka well, depth 109.5–112.5 m). (H) Gravel-dominated clast-supported conglomerate (Gcs) with erosive base and angular red claystone clasts (arrow), sandwiched between pebbly coarse-grained sandstones (Sg). Gravel-dominated braided river system (Patoka Member, Poręba). (I) SEM view of pyrogenic euhedral quartz phenocryst from Grabowa Formation (Patoka well, averaged sandy gravel sample from interval 156.0–158.9 m). (J) Gravel (Cgs) from Połomia Formation (Patoka well, depth 34 m). (K) Stromatolite from Poręba site (from Szulc et al., 2015a, b). (For interpretation of the references to colour in this figure legend, the reader is referred to the web version of this article.)

floral; Zatoń et al., 2015) and lenticular (up to 20 cm in diameter) calcite concretions. Mudstone are locally interbedded with relatively thin (up to 50 cm) horizontal and ripple-cross laminated fine-grained sandstones (Sh, Sr) and variegated palaeosol horizons (Mped) of up to 1 m thick, rich in root structures, mottles, and local small (up to a few mm) rounded carbonate nodules.

Less abundant are coarse-grained pebbly, massive, and horizontally laminated coarse-grained sandstones (Sg, Sm, Sh) with sharp erosive bases (Fig. 7G–J) and matrix- and clast-supported polymictite conglomerates (Gms, Gcs), They all occur as 3-m-thick fining-upward bodies with lenticular and tabular shapes, locally stacked onto one another in an offset manner. They can be intercalated with red and variegated mudstones with horizontal and ripple cross-laminations (Mh, Mr) and/or thin palaeosols represented by yellowish to dark red friable mudstones with poorly developed bedding (Mped).

*4.3.3.2. Interpretation.* Recognized fluvial lithofacies are considered to represent various channel and overbank sub-environments, such as a channel (sensu stricto), point bar, crevasse splay, proximal floodplain, and overbank lake. The palaeochannels can be characterized by trough cross-bedding, concave erosional bases and sandy or gravel infill often with a distinct coarse channel lag. The coarse material represents channel fills with frequent channel shifts and erosion likely related to the braided-river system. Low-angle stratification of coarse material with normal grading may indicate a downstream accretion of the straight crest bedforms, transverse bars, chute bars, and 2D dunes (Huerta et al., 2011). The occurrence of angular red claystone clasts and carbonate pedogenic nodules suggests rapid cannibalistic erosion of the relatively cohesive floodplains and associated soils (Fig. 7I) (Szulc, 2005), while the presence of dolomitic clasts indicates local erosion of older (Middle Triassic?) strata. The poorly developed bedding and cross stratification implies deposition from traction (Miall, 1996). Thin intervals of massive and pebbly sandstones were possibly deposited during single flash-flood events (North and Davidson, 2012). Unidirectional cross-stratified sandstone/mudstone heteroliths represent lateral accretion of point bars. Locally, the channel and point bar deposits enclosed by black organic mudstones typical of oxbows (Collinson et al., 2006). Oxbow claystone/mudstone intervals are interbedded with sandstones which might have formed as crevasse splays during a high-water stage. The described fining-upward trend (coarse channel sandstone → cross-stratified heteroliths sandstone-mudstone of laterally migrating point bars → fine grained oxbow claystone/mudstone) suggests a progressive abandonment of the fluvial channels indicative of a meandering river system (cf. Ielpi and Ghinassi, 2014). Local pedogenic horizons may represent poorly developed soil types, perhaps inceptisols (Varela et al., 2018).

### *4.4. Palaeosol geochemistry and mineralogy*

Thirty-four geochemical samples were collected from the Krasiejów outcrop and Patoka, Woźniki K-1, and Kobylarz wells (Ladinian–Norian interval). They represent only a clay (B) soil horizon, as it has a mean residence time long enough to disregard short-term surficial compositional changes and residual accumulation (Retallack, 2001; Sheldon et al., 2002).

Quantitative XRD analysis by Środoń et al. (2014) revealed that all samples have a very similar average composition dominated by illite/smectite (average of 33.2 wt%) and quartz (26.6 wt%), followed by carbonates (either calcite or dolomite, with average values of 10.5 and 3.8 wt%, respectively). Illite (5.9 wt%), kaolinite (4.9 wt%), hematite (2.1 wt%), chlorites (average value of 2 wt%), K-feldspars (1.6 wt%), plagioclases (mainly albite with average of 0.6 wt%) have a minor contribution to bulk mineralogy. Anatase, pyrite, siderite and goethite occur in trace amounts. For details see Supplementary Material 1.

The chemical composition of the palaeosol samples is dominated by $SiO_2$ (average of 58.3 wt%) and $Al_2O_3$ (average of 15.71 wt%). An average content of CaO is 10.97 wt% and 17 samples with CaO higher than 10%, are classified here as calcareous. The average molecular calcification ratio (defined as molar Ca + Mg/Al, see Sheldon and Tabor, 2009) is 2.18. Other major elements include FeO (Total), MgO, and $K_2O$, with averages of 6.15 wt%, 4.22 wt%, and 3.02 wt%, respectively, however, the increased $K_2O$ content is a secondary phenomenon, as discussed by Środoń et al. (2014). Trace elements are represented by Ba (average of 417 ppm), Zr, Sr, V, and Rb (averages of 196 ppm, 194 ppm, 118 ppm, and 111 ppm, respectively). Other trace elements have abundances of <100 ppm. For details see Supplementary Material 1.

The chemical data, recalculated to molar weights, were used for calculating CALMAG (Nordt and Driese, 2010) and CIA-K (Sheldon et al., 2002) weathering ratios. These models track fluxes of Ca and Mg or Na, sourced from calcium carbonate, detrital clay, and exchangeable $Ca^{2+}$ and $Mg^{2+}$ (Nordt and Driese, 2010). Standard molar weathering proxies (e.g., Chemical Index of Alternation, CIA) could not be used here because (1) a thermal event in the Cretaceous resulted in a significant potassium balance change due to smectite and partial kaolinite illitisation (Środoń et al., 2014), and (2) a depth to the calcareous horizon (Bk) which is commonly used for the palaeoprecipitation calculation could not be measured due to multiple erosive events marked by thin conglomerate (Gcs, Gms).

Calculated palaeoweathering indices vary significantly, mostly due to the variable CaO content. The CALMAG values range between 12 and 81 (average value of 37.8), corresponding to calculated Mean Annual Precipitation (MAP) between 0 and 1399 mm/yr (average of 437 mm/yr). Chemical Index of Alteration minus Potassium (CIA-K) shows a similar variation of values (between 13 and 90), giving palaeoprecipitation levels between 141 and 1229 mm/yr (average of 651 mm/yr). Samples with a lower calcification ratio (i.e. molar CaO + $MgO/Al_2O_3$ < 1) have Mean Annular Precipitations of 899 mm/yr and 1027 mm/yr for the CALMAG and CIA-K models respectively. The Mean Annual Precipitation average values have been also calculated for samples with <10 wt% of total carbonates, with MAPs of 721 mm/yr and 897 mm/yr for CALMAG and CIA-K models, respectively. Calculation results are presented in Supplementary Material 1.

### *4.5. Gravel composition*

Gravel samples from the Grabowa and Połomia formations from Patoka well include two distinctive groups of coarse grains – intraclasts and extraclasts. Intraclasts are composed of mudstones and claystones eroded from sedimentary background of the Grabowa Formation and nodular carbonates with concentric fabrics, derived from reworked caliche horizons or a nodular variety of the Woźniki Limestone Member (see Szulc et al., 2006). Extraclasts encompass the following lithologies: (1) vein quartz and quartzites; (2) meta-cherts, radiolarites, spiculites, and Algoma/Lahn-Dill-type jaspilites; and (3) kaolinized igneous rocks.

The proportion of these clasts differs between the two formations. The Grabowa Formation is characterized by abundant intraclasts (up to 90%) and rare extraclasts of vein quartz quartzites and kaolinized magmatic rocks (<10%). In addition, rare idiomorphic quartz phenocrystals are found in the sandy fraction of this formation, specifically in the Patoka Member (Fig. 7I). In contrast, the Połomia gravels are rich in extraclasts, mainly of vein quartz (54%), quartzite (16%), and chert (16%) which is consistent with studies of surface outcrop localities (see Unrug and Calikowski, 1960).

## 5. Discussion

### *5.1. Facies and depositional style*

#### *5.1.1. Playa system*

Playa deposits are known from the Lower and Upper Gypsum Beds which mark harsh conditions in arid climate. Numerous evaporitic pseudomorphoses and caliche levels imply precipitation either by evapotranspiration above the ground water table or by pedogenic process (Huerta et al., 2011). An older playa system represented by the Lower Gypsum Beds (Chrzanów Formation), have been considered as highstand deposits (HST; Aigner and Bachmann, 1992; Szulc, 2000; Feist-Burkhardt et al., 2008) and formed after a Grenzdolomite transgression in the late Ladinian. Their elevated Mg values (>5 wt%) result either from a significant admixture of local dolomitic material or early-diagenetic precipitation of dolomite (see Środoń et al., 2014).

A younger playa system, recorded as the Upper Gypsum Beds (Ozimek Evaporitic-Mudstone Member of Grabowa Formation), developed after a pluvial event of the Schilfsandstein and was induced by a return to more arid conditions in the late Carnian. This climatic shift was mega-regional, as evidenced by the distribution of the Upper Gypsum Beds over the entire Germanic Basin (Feist-Burkhardt et al., 2008), reaching Spain in the southwest (López-Gómez et al., 2002) and the UK in the northwest (Hounslow and Ruffell, 2006). The climate was hotter and drier than that during deposition of the Lower Gypsum Beds, as indicated by more extensive development of mudflats and local occurrence of palaeosols with well-developed caliche intervals (Feist-Burkhardt et al., 2008). Enhanced transpiration under these climatic conditions promoted precipitation of gypsum from deep, gypsum-supersaturated, saline groundwater (Cendón et al., 2010; Simon and Gibling, 2017a). Rare pedogenic intervals with gypsum aggregates (gypsols) could have been formed under severe arid conditions with annual precipitation as low as 250 mm/yr (Simon and Gibling, 2017a). Local sandstone and conglomerate interbeds imply a low sedimentary influx/or bypass with only sporadic erosive events. Such climatic conditions continued until the early Norian when a gilgai floodplain environment of the Grabowa Formation was established.

#### 5.1.2. Floodplain – gilgai system

Numerous, often contradictory facies and environmental models have been proposed for the bone-bearing Norian sediments. For example, for the Krasiejów site alone, Bilan (1975) has suggested a brackish (mesohaline) basin with sporadic fluvial sedimentation, whereas Dzik et al. (2000) have postulated lacustrine sedimentation with the accumulation of reptiles and amphibians in a river delta system. Szulc (2005) has ejected lacustrine interpretation of the strata and concluded instead that deposition took place under fluctuating dry to semi-dry climatic conditions with episodic rapid runoff and soil development during tranquil periods. In contrast, Gruszka and Zieliński (2008) have distinguished three sedimentary units, with two alluvial units (anastomosing and meandering) separated by a lacustrine unit with the associated pedogenic zone indicating emergence. Finally, Bodzioch and Kowal-Linka (2012), like Szulc (2005), have regarded a layer with vertebrate remains as a product of a short-lived, high-energy event. Nonetheless, Krasiejów represents only a small part of the entire floodplain system and therefore should not be considered alone, as these studies have done.

The Patoka Member of Grabowa Formation (Steinmergelkeuper) is dominated by mudstones deposited in a floodplain environment, occasionally affected by floods. The flood deposits are represented by:

(1) massive conglomerates dominated by pedogenic nodules (Gcs, Fig. 8A);
(2) massive mudstones with mm-scale calcareous clasts/nodules supported in the mud matrix (Gms, Fig. 8B); and.
(3) mudstones with internal convolutions (Fig. 8C).

As noted by Bodzioch and Kowal-Linka (2012), the bone breccia encountered in Krasiejów was hydraulically segregated, intermingled, and often fragmented (Fig. 6J) which also points to catastrophic flood events. Local soft-sediment hydroplastic deformations related to localized slumps or hyperconcentrated mudflows could also point to catastrophic run-offs, however earthquake-induced slumps and liquefaction phenomena are also possible.

An important element, which so far has not been discussed in detail are pedogenic intervals. The palaeosol horizons have thicknesses ranging between centimeters to a few meters (e.g., Patoka or Woźniki K-1 well). The mottled structure of palaeosols is common and mainly concentrated around pedogenic concretions, cracks, and slickensides which are typically formed by temporal water-table changes (pseudogleying; Licht et al., 2014, denoted also as "g"). Oxidation of the palaeosols is highlighted by the red colors developed by rubefaction. Slickensides were formed during desiccation caused by increased aridisation. Pedogenic carbonates (nodules, caliche, and laminar caps) developed during the soil drying when the rate of evapotranspiration exceeded the rate of precipitation (Zamanian et al., 2016).

Most of the recognized palaeosol intervals (both in outcrop and wells) have a distinct Bss-Bssk sequence (Fig. 6B–D) which is indicative of vertisols. Vertisols develop in alluvial plains of semi-dry tropical areas with a significant climatic seasonality, precipitation between 600 and 800 mm per year, and 3 to 6 months of annual moisture soil deficit (Retallack, 2001; Nordt and Driese, 2010). Formation of vertisols is also controlled by (1) seasonal flooding reflecting a seasonality in the catchment area (Buol et al., 2011), (2) grain-size variation, and (3) distance from river channels and avulsion belts where the water table is more stable (Licht et al., 2014).

Soils with elevated CaO values as well as numerous pedogenic carbonates (including caliche, Fig. 8E) could be classified as calcisols (e.g., Środoń et al., 2014) which often occur in dry environments. Pedogenic carbonates alone, however, are not an indicator of arid climates because they may also form in semi-arid conditions with a high climatic seasonality (Dawit, 2016), when the dissolved ions are transported during wet seasons and precipitate as calcium carbonate in dry periods (Hellwig et al., 2018).

Soil movements due to the seasonal expansion and shrinking of clay minerals can create pedoturbations responsible for local relief variations and formation of small mounds and depressions. The mounds reach up to 3 m in height and are separated by depressions with wavelengths of between 1 and 300 m (Fig. 9B). Microhighs and microlows, often truncated by fluvial deposits, are well seen in Krasiejów (Fig. 9C). The intermound areas (micro-lows) are often accompanied by thin massive claystone lenses with freshwater or brackish biota (e.g., charophyte flora; Zatoń et al., 2005). The biota, along with the presence of palygorskite, points to development of small ephemeral, most likely freshwater, lakes/ponds (Środoń et al., 2014; Szulc et al., 2017). As typical lake sediments have not been recognized in the area, small mounds, associated ephemeral ponds deposits and soil profiles could have been associated with a low energy, cohesive floodplains often inundated during flood events, typical for gilgai environment known for instance from modern Australia (Fagan and Nanson, 2004; Dixon, 2009) (Fig. 9D). The fresh groundwater was possibly recharged after episodes of catastrophic floods, as evidenced by the mottled structure of the described succession.

#### 5.1.3. Fluvial system

The alluvial architecture in the studied area is dominated by overbank deposits, whereas fluvial channels are relatively sparse, rarely exceed 10 m in thickness, and are made of meandering, braided, and possibly anastomosing fluvial systems. The fluvial channel stacking patterns can be clearly seen in the cored intervals (e.g. Woźniki K-1 or Patoka), whereas the 3D geometry is partially seen in Krasiejów, Lipie Śląskie and Poręba (Fig. 2). The meandering system is best preserved at Lipie Śląskie where trough- and tabular-bedded channel-fill sandstones, low angle cross-bedded sandstone-mudstone heteroliths of point bars, and laminated mudstones of oxbow lakes with preserved organic matter are interfingering. Very low-angle stratification of sandstone/siltstone intervals suggests deposition through lateral accretion and migration of low relief 2D dunes (Fielding, 2006). Changes in the dip angle and common reactivation surfaces indicate high-discharge events (Simon and Gibling, 2017a).

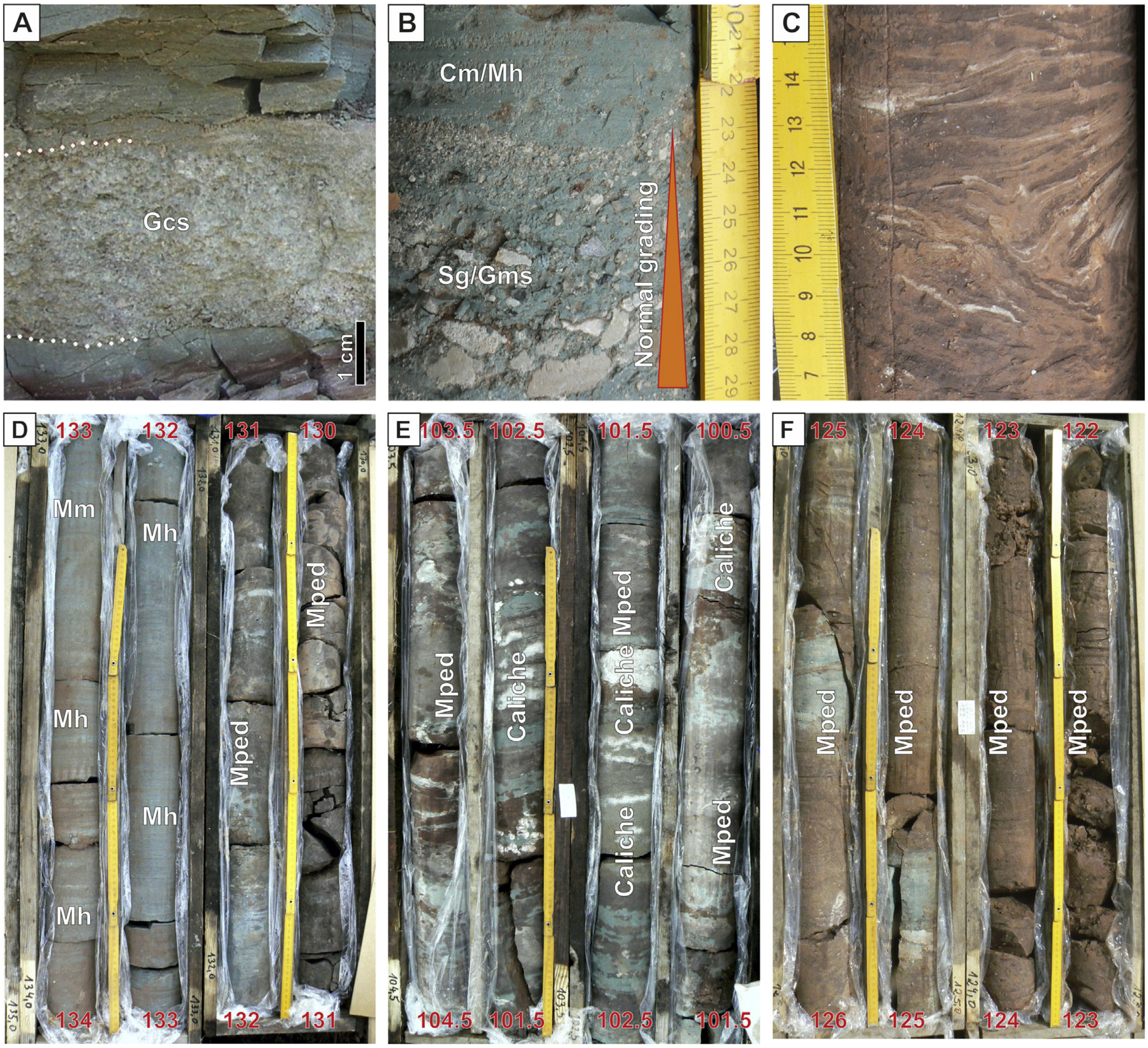


**Fig. 8.** Summary of mudstone and conglomerate facies of the Norian Grabowa Formation. (A) Clast-supported conglomerate composed of reworked pedogenic carbonate nodules, flash-flood deposit, Krasiejów outcrop. (B) Normal-graded matrix-supported conglomerate/breccia (Patoka Member, Patoka well, depth 176.8 m). (C) Mudstone with internal convolutions (Patoka Member, Kobylarz well, depth 46.0 m). (D) Pedogenic alterations (Mped) in horizontally-laminated and massive mudstones (Mh and Mm), distal floodplain facies (Patoka Member, Patoka well, depth 130.0–134.0 m). (E) Calcisols with caliche nodules and layers (Patoka Member, Patoka well, depth 101.5–104.5 m). (F) Thick red palaeosol horizon (Mped) with fine carbonate pedogenic nodules (Patoka Member, Patoka well, depth 122.0–126.0 m). (For interpretation of the references to colour in this figure legend, the reader is referred to the web version of this article.)

Determination of the sinuosity of the fluvial system at Lipie Śląskie is impossible due to limited exposure, however, this parameter can be estimated using the empirical relation of Williams (1986) and the maximum observed channel depth. As the depth of fluvial channels in Lipie Śląskie does not exceed 2 m, this means that the meander belt is modelled as being approximately 450 m wide. The river sinuosity may well have been strongly affected by the river bank vegetation, as indicated by accumulation of small and large plant remnants (Fig. 7F), including tree trunks as long as 14 m. Dense bank vegetation would have reduced the erodibility of the river through restricting channel mobility, which ultimately leads to choking off of weaker channels and creation of the oxbows, rather than redistribution of the river flow into fewer channels with higher velocities (Tal et al., 2004). The water discharge varied, as indicated by choke-off channel deposits with the Bouma-like sequence (massive sandstone → horizontal laminated sandstone → ripple cross-laminated fine sandstone), implying a relatively rapid sedimentation from sand-loaded flows (Fig. 7A). The presence of variously shaped oncoid beds (low-energy and stagnant water conditions) and stromatolites (Fig. 7K) under breccias (high-energy episodes) also suggests a variable water discharge (Tałanda et al., 2017). The sandstones are relatively well sorted, and contain rounded sand grains and charcoaled organic matter (see Marynowski and Simoneit, 2009), suggesting a long transport distance (Kubik et al., 2015). However, episodic floods eroded nearby floodplains bringing local material, such as pedogenic nodules or dolomite clasts. The meandering river system model for Lipie Śląskie is presented in Fig. 9A. Transition from cross-laminated sandstones to organic-rich horizontally laminated mudstones is also seen in Woźniki K-1 well (basal part of Schilfsandstein at 82 m) and Patoka well (at 145–159 m) (Figs. 3,5).

The braided river system is likely exposed in the Poręba outcrop (SE part of the studied area). The architectural elements include vertically amalgamated channel bodies with multistorey coarse-grained and pebbly sandstones (Sg and Gms) and polymictic conglomerates with dolomite/claystone clasts and oncoids (Gcs, Gms; Fig. 7H). These sedimentary features can be attributed to proximal sand and gravel dominated parts of the system, fed by episodic floods. Alternatively, the coarse material may also be associated with local alluvial fans developed at the foot of locally elevated areas. The presence of alluvial fans

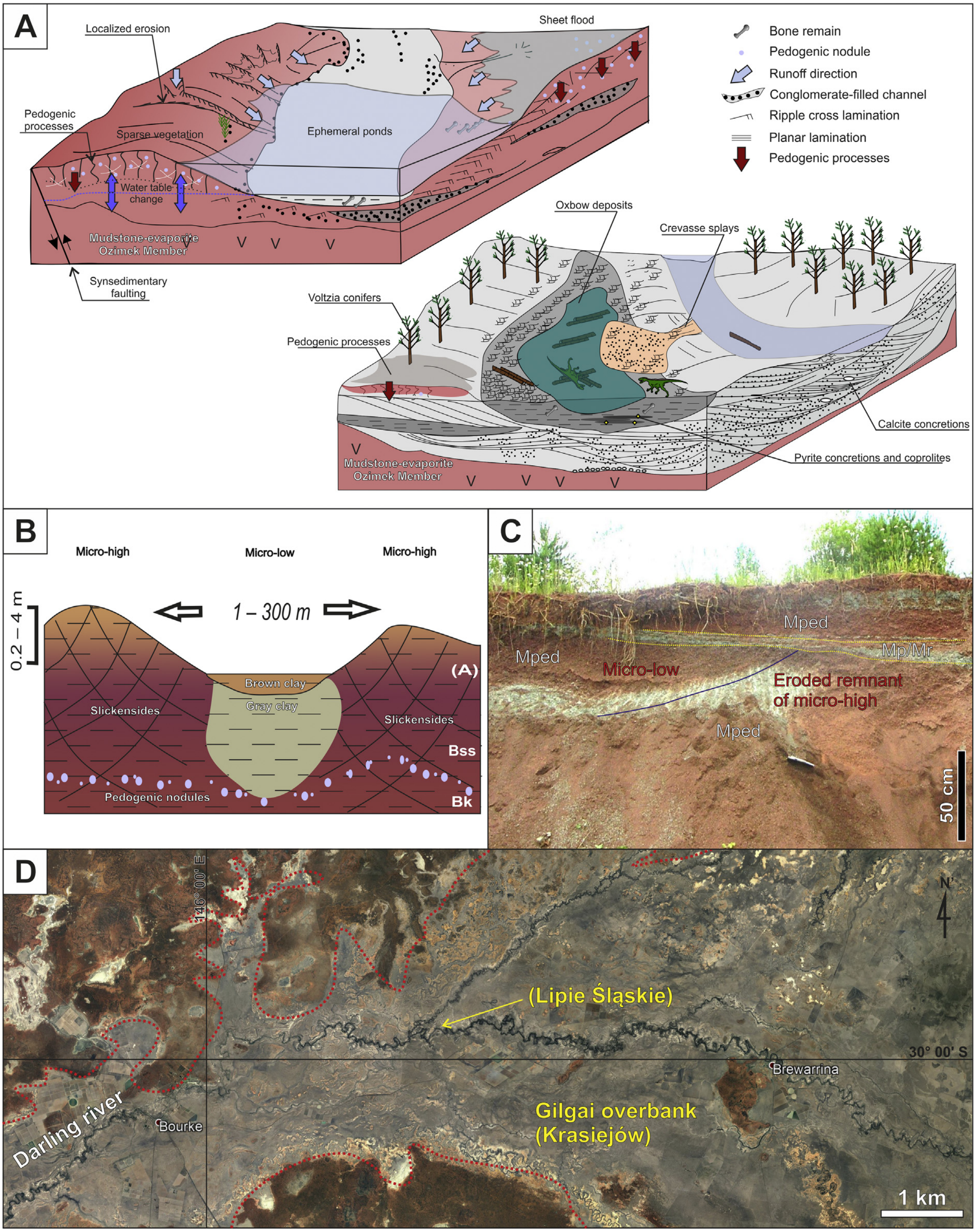


**Fig. 9.** (A) Schematic illustration of the gilgai palaeoenvironment at Krasiejów (upper model) and meandering river system at Lipie Śląskie (lower model) (cf. Bodzioch and Kowal-Linka, 2012; Szulc et al., 2015a). (B) Gilgai relief (after Dixon, 2009, modified). (C) An example of gilgai relief in Krasiejów. (D) Satellite image of the Darling river in Northern Basin (Murray-Darling Basin, SE Australia), as a modern analogue for the Norian gilgai environment in Upper Silesia. The dryland river system encompasses a complex channel system characterized by broad alluvial plains (red dashed line) with well-developed vertisols and gilgai microrelief. Highly seasonal climate is driven by wet La-Niña and dry El Niño. (For interpretation of the references to colour in this figure legend, the reader is referred to the web version of this article.)
(Source: Google Earth, 2018.)

and braided rivers in the studied area has been postulated by Pieńkowski (1988).

In addition to meandering and braided system, a low-energy fluvial system could have also existed, especially in the distal parts of the Silesian Keuper system. Gruszka and Zieliński (2008) proposed a silt-loaded anastomosed river with low energy, flowing to the north-west. They recognized fluvial palaeochannels with an anabranching channel pattern and filled with siltstones. Such systems develop in a relatively high aggradation environment with a constant base level rise, controlled mainly by tectonic subsidence. The aggradation rate may be assessed by stacking patterns of soil horizons (see Kraus, 1999). Most of the palaeosol horizons in the analysed boreholes represent a cumulative palaeosol type (Kraus, 1999), indicating pedogenesis rates higher than sediment aggradation and development in some distances from the avulsion belt. In the Krasiejów site, however, a thin initial soil (probably inceptisols) sandwiched between laminated mudstones indicates higher aggradation rates.

Although Gruszka and Zieliński (2008) suggested a low-gradient and low-energy environment, numerous coarse-grained sandstones and conglomerates composed of outwashed pedogenic nodules as well as disarticulated bone fragments indicate high energy events likely related to unconfined flash-floods and localized steeper gradients. Various palaeotransport directions visible in the Krasiejów site (e.g., Fig. 6H) also point to variable topography.

The presence of large-scale cross-stratified structures in the Krasiejów outcrop may be associated with bedload transport and deposition of the sand-size (or even larger) clay aggregates which hydrodynamically differ from denser and smaller quartz particles (see Simon and Gibling, 2017b). Such aggregates have been documented in analogue Australian alluvial environments of Cooper and Diamantina Rivers floodplains (Rust and Nanson, 1989) representing an important fraction of the alluvial plain deposits. Formation of mud aggregates was enhanced by the abundance of swelling-type clays such as smectite, abundant in the Silesian Upper Triassic vertisol profiles (Środoń et al., 2014) and as such these could be incorporated into migrating point bars (Simon and Gibling, 2017b).

Anastomosing rivers are known from the semi-arid settings of Australia (Makaske, 2001; Fagan and Nanson, 2004). Such system can coexist with braided-channel system even in the low-gradient environments, especially where the mud-pellet bedload transport dominates (cf. Nanson et al., 1986).

### *5.2. Tectonic control on distribution of fluvial deposits*

The spatial and temporal distribution of Upper Triassic fluvial deposits in the studied area can be linked to the development of tectonically controlled depressions. Although the orientations of individual river tracks have proved impossible to reconstruct, most fluvial deposits are bound to Kraków-Lubliniec Fault (Fig. 1C) which is one of the major lineaments in the area (Morawska, 1997) and marks the boundary between the ancestral Upper Silesian and Małopolska Terranes. The fault was particularly active in the late Palaeozoic, however there is also evidence of its reactivation in the Triassic (Szulc, 2000). Norian spring-related carbonates (Woźniki Limestone Member of the Grabowa Formation, Fig. 1C) located along the Kraków-Lubliniec fault system have a clear hydrothermal oxygen isotopic signature (Słowakiewicz, 2003; Szulc et al., 2006), suggesting that the fault was active in the Norian and possibly throughout the entire late Triassic. The possible block movements in the Norian (and possibly earlier during deposition of the Carnian Schilfsandstein clastics) could have therefore resulted in the lateral facies variations, hiatuses and discordances and changes in accommodation space required for the preservation of the system. Yet, the uplifted, fault-controlled areas were likely eroded by incised river systems and sourced alluvial fans or the proximal braided-fluvial system (see Dittrich, 1989).

In fault-controlled valleys and rifts, the abundance of multistorey channels increases proximal to active faults whereas palaeosols tend to be preserved distal to the fault system. This is analogous to the Pliocene-Pleistocene Rio Grande Rift system in the United States (Mack and Madoff, 2005) and Upper Triassic Ischigualasto Formation in Argentina (Currie et al., 2009). Coarse-grained and more commonly stacked and amalgamated facies can be found in Upper Silesia, albeit with low thicknesses. The coarse-grained sediments are more common in the SE part of the studied area and close to the Lubliniec fault. In the northwestern distal part of the system, fluvial deposits are sandwiched by relatively thick (>10 m) overbank deposits, suggesting a discrete ribbon shape of the channel belts, further indicating a relatively high accommodation space and sediment supply (Huerta et al., 2011). Discrete ribbons were more likely prone to sediment plugging and avulsions. This is similar to patterns proposed for the Triassic fluvial system of the northern Permian Basin (McKie, 2014). Conversely, well-preserved stacked palaeosol intervals point to a very low sediment supply. As such, the palaeolandscape, if controlled by tectonics, had only a minor impact on the Norian river track system development in the area (Szulc et al., 2015b).

Relatively weak tectonic activity in the Norian was probably linked with early Cimmerian block tectonism which was related to the rifting in the Western Tethys (Szulc, 2000) and its effect in the Upper Silesia region was probably minor. A clearer pulse of rejuvenation of the landscape took place in the Rhaetian when compositionally mature conglomerates and coarse-grained sandstones of the Połomia Formation accumulated (Fig. 9J). The base-Rhaetian disconformity in Upper Silesia could correspond to the regional D6 unconformity in Germany (Beutler et al., 2005) or Kimmerian II unconformity in the UK (Hounslow and Ruffell, 2006).

### *5.3. Sediment supply – provenance and palaeotransport*

The qualitative analysis of the coarse-grained fraction from the Patoka well shows significant compositional differences between conglomerates of the Grabowa (Norian; Fig. 7G, H) and Połomia (Rhaetian; Fig. 7J) Formations. The compositional maturity generally increases towards the Rhaetian, which can be independently confirmed by an increase in the Zr/Al ratio (Środoń et al., 2014), which implies enhanced hydraulic sorting. Local variations in the thickness of fluvial deposits of the Grabowa Formation and the relatively uniform composition of grains dominated by intraclasts and kaolinized effusive extraclasts indicate intensive erosion and aggressive chemical weathering of the immature siliciclastic material in a seasonal, semi-arid climate.

The provenance and transport directions of the Grabowa Formation coarse intervals remain controversial. As the northern massifs (such as Scandinavia) could have supplied detritus to the NE part of the Germanic Basin, the study area was more likely sourced from the western, southern, and/or eastern directions (Fig. 1B). Based on lateral patterns in the distribution of the siliciclastic strata, Pieńkowski et al. (2014) proposed eastern and southern zones as sources for the Upper Triassic–Lower Jurassic interval. In contrast, Sm-Nd isotope analysis by Konieczna et al. (2015) indicates that the Saxothuringian zone of the Variscan orogeny (or more broadly Sudety Land; sensu Pieńkowski et al., 2014) was the primary source of detritus. Based on available geochemical data from the studied area (Środoń et al., 2014), a gradual increase in Cr/Ti ratio could indicate a shift in the source from more geochemically mafic towards more basic sources over the Carnian–Norian period. This is supported by the presence of idiomorphic quartz phenocrysts, recognized in the sand fraction of the Patoka Member in the Patoka well (Fig. 7I), which can be interpreted as a residuum of completely weathered matrix of acidic rhyolitic material.

The Połomia gravels are generally characterized by a diverse composition of pebbles when compared to the Grabowa Formation. Many of these lithologies are not recognized in the Fore-Carpathian and Lublin Land areas which are widely accepted as main source terrains for the Upper Silesian Keuper and Lower Jurassic. Ordovician glauconitic limestone pebbles (recently radiometrically dated by the K-Ar method ca. 465 Ma, Banaś; *personal communication, January 2018*) are common in Sloboda Miocene conglomerates which were sourced from the Lower San River Massif (Fig. 1B) located northwards in the Ukrainian Carpathians (Oszczypko et al., 2012). In contrast, the presence of clasts of Algoma/Lahn Dill-type jaspilites (known from the Eastern Carpathians) and various effusive volcanics strongly suggests that the main source area was the Moeasian Platform, located in a pre-Carpathian position in the late Triassic (Tari et al., 2012). In the latter scenario, the hypothesized drainage system would be determined by a long-distance fluviatile delivery along the faulted southern Laurasian coast. This hypothesis is given added credence by K-Ar ages of detrital micas from the Arnstadt Formation in central Germany whose ages are linked with the "Panafrican" source located at the current position of southern Poland or Slovak Republic (Paul et al., 2009).

### 5.4. Climatic control

As tectonism is hypothesized to play only a minor part in the sedimentary pattern of the studied area, the development of the Upper Silesian floodplain ("gilgai") – playa system is attributed to climatic variations. Dry periods are marked by the presence of evaporites (Lower and Upper Gypsum Beds), while wet periods were accompanied by an increase in sediment supply and moving of the proximal facies towards the central part of the German basin (Carnian Schilfsandstein and Rhaetian).

The Carnian Pluvial Episode (CPE) is recognized across the entire Germanic Basin in the humid intervals (Feist-Burkhardt et al., 2008). This event is recorded in the Upper Silesia region as the fluvial Schilfsandstein encountered in both the Woźniki and Koziegłowy WB-3 wells, dominated by fluvial facies with poorly preserved hydromorphic soils of proximal floodplains. The reasons for increased humidity in the middle Carnian are still debated: Kozur and Bachmann (2010) attributed the CPE in the Germanic Basin to tectonic factors, as the monsoonal circulation was strengthened by the uplifted rift shoulder of the Caledonides between Scandinavia and Greenland. In addition, the influence of large volcanic eruptions on climate cannot be ruled out (e.g., related to the formation of Wrangellia Igneous Province; Tanner, 2018).

The internal architecture of the Steinmergelkeuper floodplain in Upper Silesia can also be explained by climatic changes, as the local m-scale alternation of flood-related deposits and palaeosols indicates a short-term recurrence of humid and arid periods respectively. Similar cyclicity in the correlated Norian central playa sediments, Central Germany, was interpreted as the result of an orbitally modified monsoonal circulation (e.g., Reinhardt and Ricken, 2000; Vollmer et al., 2008) this interpretation is uncertain for sediments in this study. Also, the appearance of fluvial channels in the relatively distal Patoka-1 well could be linked to climate wetting and the associated progradation of the coarse proximal facies towards the basin center. Finally, the thickness changes of zones and annuli in *Metoposaurus* femora bones have been attributed to a high climate seasonality (Konietzko-Meier and Sander, 2013).

An increase in the sediment maturity (Grabowa vs. Połomia Formations) and in the abundance of kaolinite and smectite in the Upper Norian (Środoń et al., 2014) and Rhaetian sediments (Pieńkowski et al., 2014) points to a gradual onset of humid climate across the Norian/Rhaetian boundary. This was possibly associated with a slow northward drift of Silesia as demonstrated by magnetostratigraphic studies (e.g., Nawrocki et al., 2015) which corresponds to a transition from subtropical convergence zone (possibly strongly affected by a monsoon circulation system) to more temperate latitudes.

### 5.5. Pedogenesis and the climatic record

Palaeosols are an important tool in reconstructing palaeolandscapes and environmental processes, as they record atmospheric conditions and the evolution of floodplains (cf., Licht et al., 2014; Dawit, 2016). Pedogenesis takes place in periods of landscape stability when the rate of sedimentation is lower than the rate of soil formation (Kraus, 1999), and the level of pedogenesis is a function of the mean annual precipitation (MAP; mm) and mean annual temperature (MAT; °C; Sheldon et al., 2002).

The majority of the analysed palaeosol horizons are calcareous and consequently their CALMAG and CIA-K ratios as well as MAPs are relatively low, between 300 and 500 mm/yr (mean: 401 mm/yr, standard deviation of $\pm$108 mm/yr and $\pm$ 172 mm/yr for CALMAG and CIA-K models respectively; Fig. 10). These values are in agreement with those presented in an idealized Pangean climatic model for the inland position in the late Triassic (350–750 mm/yr; Kutzbach, 1994) as well as the General Circulation Models for a summer-wet biome zone (which the Upper Silesia belonged to; Sellwood and Valdes, 2006). Sixteen samples with low carbonate content (<10%, see Supplementary Material 1 and Środoń et al., 2014) yield MAPs ranging from 500 to 1154 mm/yr (average 721 mm/yr) and these values fall within the range obtained for Upper Triassic Chinle Formation vertisols in eastern New Mexico (701 $\pm$ 108 mm/yr; Nordt and Driese, 2010).

One should remember that mean annual precipitation values will have differed geographically as a function of the distance from the Tethys ocean, monsoonal activity strength, and palaeo-elevation. Topographic roughness of the areas due to variable landscape could be also responsible for increased rainfalls in the hinterlands due to orographic precipitation (e.g., Fig. 13.15 in Feist-Burkhardt et al., 2008). Additionally, the ocean-land configuration in the late Palaeozoic/early Mesozoic created a significant climatic gradient, with maximum precipitation located near the Tethys coast and severe continental climate in the continental interior (more likely arid; Kutzbach and Gallimore, 1989; Kutzbach, 1994; Wang et al., 2014). The role of the Vindelican and/or Moesian lands in affecting the atmospheric palaeocirculation in the studied region is unknown. Recently, Onoue et al. (2018) have suggested that the mid-Norian pluvial event resulted from the uplift of the Cimmerian Mountains, which affected a global atmospheric circulation and enhanced rainfall in the western part of the Tethys domain.

The palaeoposition of the Upper Silesia region within the Germanic Basin can potentially be compared with modern analogues from Australia, with the Lower and Upper Gypsum Beds corresponding to the playa/alluvial zone located in the north-eastern portion of the Lake Eyre (Cooper Creek in the Channel Country of Queensland). There, rainfalls and runoffs are currently controlled by the monsoonal activity influenced by the El Niño-Southern Oscillation, with wet La-Niña and dry El Niño conditions, giving the mean annual precipitation of only 127 mm/yr (Cendón et al., 2010). Conversely, localities closer to the Great Divine Range have higher annual precipitation of approximately 500–600 mm/yr (Australian Bureau of Meteorology website, http://www.bom.gov.au/climate/data/ 2018), which results from orographic precipitation and generates dry-land type rivers (e.g., the Darling river) and extensive floodplains with well-developed vertisols (Fig. 9D).

Analysis of two samples from Schilfsandstein palaeosols produces higher annual palaeoprecipitation values of approximately 1143 mm for the CALMAG model and 1050 mm/yr for the CIA-K model. These may be overestimated because these palaeosols are not classical vertisols, but soils developed in frequently inundated floodplains.

One should be careful in accepting that Mean Annual Precipitation (MAP) values are definitive for producing late Triassic palaeoclimatic reconstructions, as large variations in Ca and Mg concentrations significantly underestimate MAP. Although CALMAG-based palaeoprecipitation estimations for vertisols are more accurate than CIA-K-based ones (Nordt and Driese, 2010; Adams et al., 2011), the differences in MAP calculation may be large if samples were taken from inappropriate soil horizons or if the B horizon is <1 m thick (Adams et al., 2011).

Temperature determination from the chemical data using potassium (e.g., Sheldon and Tabor, 2009) was not possible due to post-depositional incorporation of K into sediments (Środoń et al., 2014).

### 5.6. Taphonomical implications

Numerous palaeontological sites in the Upper Silesia region have a great potential in contributing to the evolutionary analysis of various

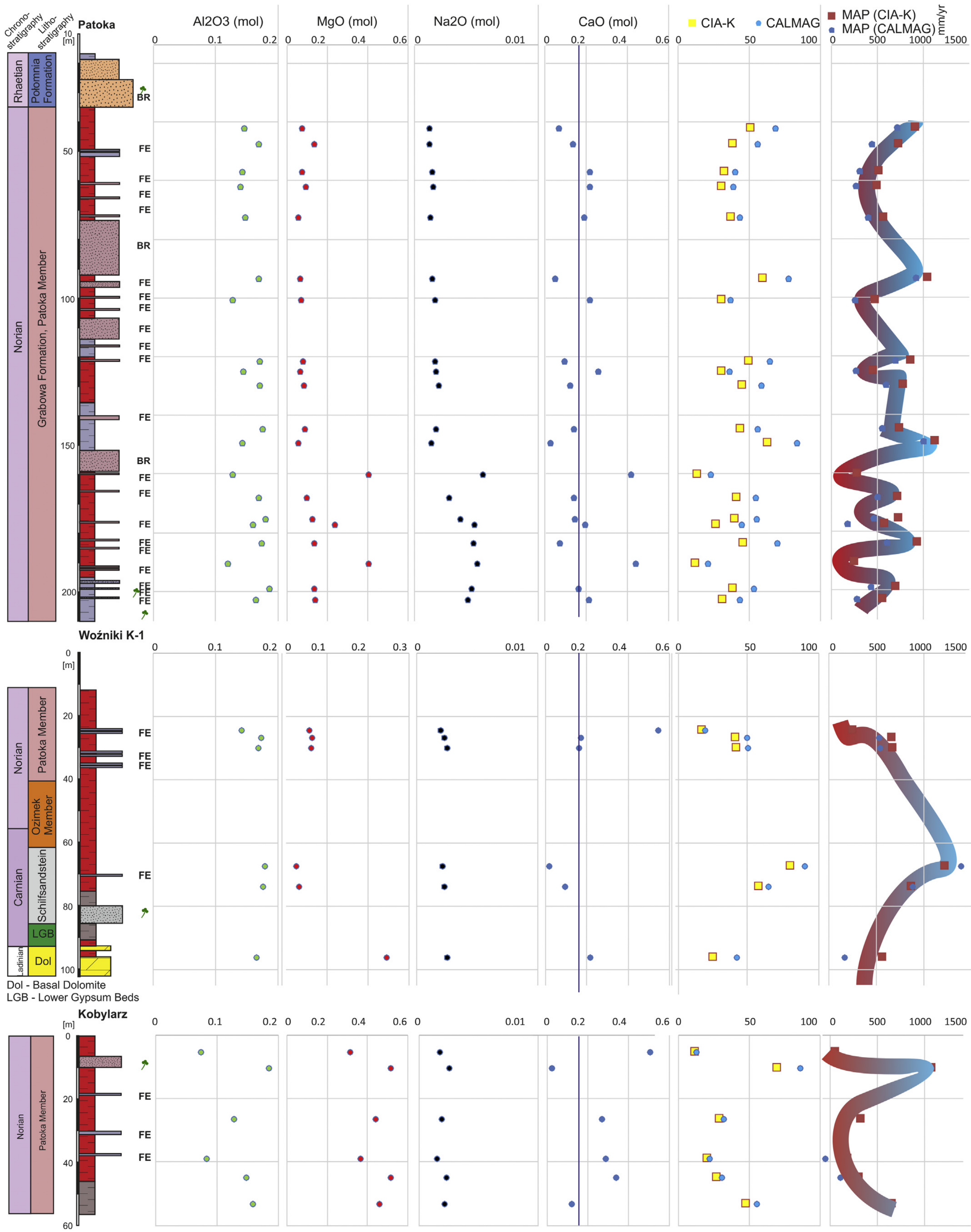


**Fig. 10.** Geochemical data for selected palaeosol horizons from Patoka, Woźniki K-1, and Kobylarz wells. $Al_2O_3$, MgO, $Na_2O$, and CaO are in wt % / molecular weights. Molecular ratios of CALMAG and CIA-K and Mean Annular Precipitation (MAP) were calculated following Nordt and Driese (2010) and Sheldon et al. (2002). MAP results for samples rich in CaO (>10 wt%, 0.17 molar) should be taken with caution as they may be underestimated. The "vertisol" range is between 600 and 800 mm/yr, typical for vertisol-dominated environments (Retallack, 2001; Nordt and Driese, 2010). Most of the samples with CaO below 10% are within the vertisol range.

groups of animals such as large vertebrates. Although some authors claim bone accumulations are in situ (e.g., Dzik and Sulej, 2007), osteohistological and diagenetic analyses of bone fragments combined with sedimentological studies of the bone-bearing horizons point to a secondary accumulation of the skeletal material (Szulc, 2005; Bodzioch and Kowal-Linka, 2012; Konietzko-Meier and Klein, 2013; Szulc et al., 2017). As demonstrated above, although the gilgai environment was relatively stable, thin intercalations of conglomerates with pedogenic nodules implicate occasional catastrophic floods which were responsible for the accumulation of bone material in small topographic depressions and subsequent quick burial. Bodzioch and Kowal-Linka (2012) have identified two bone populations with different diagenetic histories within the richest bone level in Krasiejów, indicating that the skeletons were transported from different parts of the gilgai environment. The post-depositional disintegration of bone material was likely inhibited by elevated alkalinity at the early stage of diagenesis (Dzik and Sulej, 2007). The enhanced alkalinity was sourced from the weathering of the highly calcareous (CaO > 10%) host rock. Accordingly, the greatest potential for the bone preservation is in the flood-related deposits (both conglomerates and mud-flow deposits).

### 5.7. Vertical depositional model

The construction of a depositional model for the studied area is not a trivial task, as demonstrated by numerous, often contradictory, works discussing sedimentology and stratigraphy of the Carnian–Rhaetian sediments of Silesia region (e.g., Bilan, 1975; Dzik, 2001; Szulc, 2005; Dzik and Sulej, 2007; Gruszka and Zieliński, 2008; Bodzioch and Kowal-Linka, 2012; Pieńkowski et al., 2014; Fijałkowska-Mader et al., 2015; Racki and Szulc, 2015, Racki and Lucas, 2018). The difficulty has arisen from the facies variability and scarcity of outcrops and cored wells. In addition, two different methodological approaches (sedimentological vs. palaeontological) have been used, leading to conflicting interpretations.

The vertical arrangement of the facies associations within the Upper Triassic succession records a long-term transition from playa to gilgai environments, interrupted by the development of short-lived fluvial systems which can be interpreted in terms of changes in accommodation space and sediment supply. Depositional models for SE Germany in the Carnian, Norian, and Rhaetian were constructed based on progradation and retrogradation of facies belts (terminal alluvial plains, playa margin, and playa lake), which were controlled chiefly by the strength of monsoonal activity and base level rise/fall (Hornung and Aigner, 1999, 2002a, 2002b; Reinhardt and Ricken, 2000). A similar interaction of alluvial and lacustrine environments has been documented in Upper Triassic deposits of the Travenanzes system in the Italian Dolomites (Breda and Preto, 2011). There, remobilization of the 'stored sediment' in basinal margins was interpreted to have been associated with local erosion and progradation of the proximal sandstone facies and mudflats developed in the playa lake bottom. These were in turn linked to periods of low base level which resulted from significant evaporation of the playa lake during arid climatic stages. Carbonates were formed during high playa lake levels and transitions from humid to arid phases. Because of the relatively high base level, erosion was minimal and therefore pedogenic processes were widespread. Catastrophic events such unconfined flows (possibly developed as sheet floods) was associated with the initial stages of base level fall associated with arid climatic conditions. The localized uplift of tectonic blocks and the resultant erosion and sediment supply also attributed to localized changes in the sedimentary architecture. Isolated fluvial architectural elements in the Patoka well may represent isolated short-lived, ribbon-shape, sand-dominated channel belts which could have formed during a high sediment supply and high accommodation space with a relatively high avulsion frequency (Bryant et al., 1995), although the latter feature is difficult to recognize in the sedimentary record (Huerta et al., 2011). Extensive floodplains with stacked soils and solitary, scattered channels may be indicative of relatively low accommodation space and low sediment supply. This provided a stable environment controlled by a climate seasonality which was an optimal habitat for numerous groups of animals. The high seasonality of the climate, responsible for triggering catastrophic run-off, had also great potential for taphonomic preservation of the vertebrate bones (Bodzioch and Kowal-Linka, 2012).

## 6. Conclusions

Results of integrated sedimentological and geochemical study of the Keuper strata from SE Poland can help in our understanding of the climate driven changes of terrestrial environments through the late Triassic and their impacts on vertebrate evolution. The analysed succession starts with Carnian inland playa deposits with gypsum nodules and weakly developed soils, shortly interrupted by fluvial facies of the Schilfsandstein, likely associated with mid-Carnian Pluvial Event (CPE). With the beginning of Norian, a shift to semi-dry climate resulted in widespread vertisoles and flood-related deposits. Palaeosol development was facilitated by a very low sediment supply, low accommodation space, and reduced tectonic subsidence. The pedogenic processes were dominated by vertisation and rare hydromorphism. The soil movements, enhanced by enrichment in swelling clay minerals were responsible for development of a system of micro-lows and micro-highs, diagnostic of a gilgai relief. Such relief had an influence on the distribution and extent of small freshwater ponds and the direction of floods.

The Keuper fluvial system is volumetrically subordinate and is represented by braided, meandering, and potentially silt-dominated anastomosing river deposits. Braided and meandering river systems predominated in the proximal, southern part of the basin, where local gradients were likely higher. In more distal parts of the basin (north and north-west), where overbank deposits prevailed, low-energy silt-loaded anastomosing/braided river systems and ephemeral streams could have also developed, especially during occasionally wetter seasons. Gravel and sand transport was dominant in the proximal part of the studied system, whereas mud-aggregate bedload transport and unconfined flow processes such as sheet-floods prevailed in distal settings. All environmental changes through the late Triassic were mostly controlled by climatic factors and to a lesser degree by synsedimentary tectonism associated with the regional Lubliniec fault system. The uplifted blocks, likely composed of Middle-Triassic marine carbonates, were a source of the local material incorporated into floodplain deposits. The change in the maturity and composition of the gravel fraction between the Norian Grabowa and Rhaetian Połomia Formations can be attributed to the change in provenance. The dominance of extraclasts within the latter formation points to a long-river track fed from the south-east (River San Massif and/or Moesian Platform).

The geochemical analyses of vertisol samples from the Grabowa Formation enabled calculating Mean Annual Palaeoprecipitation of 721 mm/yr (±108 mm/yr). The calcisols have lower values, but they are still in accordance with numerical-based palaeoclimatic models for the 40°N in the late Triassic. High climatic seasonality is reflected in the alteration of well-developed vertisols and flood-related deposits. The geochemically-derived Mean Annual Precipitation (MAP) values as well as facies arrangement can be compared with modern SE Australia lowlands characterized by semi-arid conditions and a high climatic seasonality. Modern Australia environment can thus be regarded as a basic model for studying palaeoecology of various groups of animals including large vertebrates found in Fossillagerstätten-type bone beds in the Upper Silesia region.

Supplementary data to this article can be found online at https://doi.org/10.1016/j.sedgeo.2018.11.005.

## Acknowledgements

This research was supported by Polish National Research Grant (N307 11703) led by professor Grzegorz Racki from University of Silesia in Katowice. We would like to thank him for his encouragement and constructive criticism of the manuscript. KJ would like to thank Natalia Wasielka (Durham University, UK) for comments which improved first draft of the paper. We would like to thank professor Jan Środoń (Institute of Geological Sciences, Polish Academy of Sciences) for providing geochemical and mineralogical data for palaeosol characterization. Thanks go to Waldemar Bardziński (Silesian University) for his assistance in data collection and core photographs. We would like to thank Alex Finlay PhD (Chemostrat Ltd. Welshpool, UK) for reading the manuscript, language-proof and helpful advice. We also acknowledge the valuable comments of Reviewers Beata Gruszka and Mark Hounslow. The comments of Editor Jasper Knight helped to improve the manuscript.

## References

Adams, J.S., Kraus, M.J., Wing, S.L., 2011. Evaluating the use of weathering indices for determining mean annual precipitation in the ancient stratigraphic record. Palaeogeography, Palaeoclimatology, Palaeoecology 309, 358–366.

Aigner, T., Bachmann, G.H., 1992. Sequence-stratigraphic framework of the German Triassic. Sedimentary Geology 80, 115–134.

Antczak, M., Bodzioch, A., 2018a. A description of Late Triassic isolated fish scales from Krasiejów, Poland. Paleontological Research 22, 91–100.

Antczak, M., Bodzioch, A., 2018b. Ornamentation of dermal bones of *Metoposaurus krasiejowensis* and its ecological implications. PeerJ 6, e5267(1). https://doi.org/10.7717/peerj.5267.

Benton, M.J., Forth, J., Langer, M.C., 2014. Models for the rise of the dinosaurs. Current Biology 24, R87–R95.

Beutler, G., Dittrich, D., Dockter, J., Ernst, R., Etzold, A., Farrenschon, J., Freudenberger, W., Hauschke, N., Heunisch, C., Kelber, G., Knapp, G., Lutz, M., Nitsch, E., Oppermann, K., Schubert, J., Schulz, E., Schweizer, V., Seegis, D., Tessin, R., Vath, U., 2005. Keuper, Starigraphie von Deutschland, Courier Forschungsinst. Senckenberg, Frankfurt (296 pp.).

Bilan, W., 1975. Profil retyku w Krasiejowie koło Opola (The Rhaetic profile in Krasiejów near Opole). Zeszyty Naukowe AGH, Geologia 1, 13–19 (In Polish, with English summary).

Bodzioch, A., Kowal-Linka, M., 2012. Unraveling the origin of the Late Triassic multitaxic bone accumulation at Krasiejów (S Poland) by diagenetic analysis. Palaeogeography, Palaeoclimatology, Palaeoecology 346, 25–36.

Breda, A., Preto, N., 2011. Anatomy of an Upper Triassic continental to marginal-marine system: the mixed siliciclastic-carbonate Travenanzes Formation (Dolomites, Northern Italy). Sedimentology 58, 1613–1647.

Bryant, M., Falk, P., Paola, C., 1995. Experimental study of avulsion frequency and rate of deposition. Geology 23, 365–368.

Buol, S.W., Southard, R.J., Graham, R.C., McDaniel, P.A., 2011. Soil Genesis and Classification. Wiley Blackwell, Oxford (543 pp.).

Cendón, D.I., Larsen, J.R., Jones, B.G., Nanson, G.C., Rickleman, D., Hankin, S.I., Pueyo, J.J., Maroulis, J., 2010. Freshwater recharge into a shallow saline groundwater system, Cooper Creek floodplain, Queensland, Australia. Journal of Hydrology 392, 150–163.

Cohen, K.M., Finney, S.C., Gibbard, P.L., Fan, J.-X., 2013. The ICS International Chronostratigraphic Chart. Episodes 36, 199–204 updated.

Collinson, J.D., Mountney, N.P., Thompson, D.B., 2006. Sedimentary Structures. Terra Publishing, Enfield (292 pp.).

Currie, B.S., Colombi, C.E., Tabor, N.J., Shipman, T.C., Montañez, 2009. Stratigraphy and architecture of the Upper Triassic Ischigualasto Formation, Ischigualasto Provincial Park, San Juan, Argentina. Journal of South American Earth Sciences 27, 74–87.

Dawit, E.L., 2016. Paleoclimatic records of Late Triassic paleosols from Central Ethiopia. Palaeogeography, Palaeoclimatology, Palaeoecology 449, 127–140.

Dittrich, D., 1989. Der Schilfsandstein als synsedimentär-tektonisch geprägtes Sediment – eine Umdeutung bisheriger Befunde. Zeitschrift der Deutschen Geologischen Gesellschaft 140, 295–310 (In German, with English summary).

Dixon, J.C., 2009. Aridic soils, patterned ground and desert pavements. In: Parsons, A.J., Abrahams, A.D. (Eds.), Geomorphology of Desert Environments. Springer, pp. 101–122.

Dzik, J., 2001. A new Paleorhinus fauna in the early Late Triassic of Poland. Journal of Vertebrate Paleontology 21, 625–627.

Dzik, J., Sulej, T., 2007. A review of the early Late Triassic Krasiejów biota from Silesia, Poland. Palaeontologia Polonica 64, 3–27.

Dzik, J., Sulej, T., Kaim, A., Niedźwiedzki, R., 2000. Późnotriasowe cmentarzysko kręgowców lądowych w Krasiejowie na Śląsku Opolskim (A late Triassic tetrapod graveyard in the Opole Silesia (SW Poland)). Przegląd Geologiczny 48, 226–235 (In Polish, with English summary).

Fagan, S.D., Nanson, G.C., 2004. The morphology and formation of floodplain-surface channels, Cooper Creek, Australia. Geomorphology 60, 107–126.

Feist-Burkhardt, S., Götz, A.E., Szulc, J., Aigner, T., Borkhataria, R., Geluk, M., Haas, J., Hornung, J., Jordan, P., Kempf, O., Michalík, J., Nawrocki, J., Reinhardt, L., Ricken, W., Röhling, H.G., Ruffer, T., Török, A., Zuhlke, R., 2008. Triassic. In: McCann, T. (Ed.), The Geology of Central Europe. The Geological Society, London, pp. 749–821.

Fielding, C., 2006. Upper flow regime sheets, lenses and scour fill: extending the range of architectural elements for fluvial sediment bodies. Sedimentary Geology 190, 227–240.

Fijałkowska-Mader, A., Heunish, C., Szulc, A., 2015. Palynostratigraphy and palynofacies of the Upper Silesian Keuper (southern Poland). Annales. Societatis Geologorum Poloniae 85, 637–661.

Franz, M., 2009. A multistratigraphic approach for the Keuper (Upper Triassic) in the eastern Central European Basin (D, PL) and the Danish Basin (DK, S). In: Haczewski, G. (Ed.), Abstracts and Field Guide. 6th Annual Conference of SEPM-CES SEDIMENT 2009 17.

Gruszka, B., Zieliński, T., 2008. Evidence for a very low-energy fluvial system: a case study from the dinosaur-bearing Upper Triassic rocks of Southern Poland. Geological Quarterly 52, 239–252.

Gunatilaka, A., Mwango, S., 1987. Continental sabkha pans and associated nebkhas in southern Kuwait, Arabian Gulf. In: Frostick, L.E., Reid, I. (Eds.), Desert Sediments: Ancient and Modern. Geological Society Special Publications, London, pp. 187–203.

Hellwig, A., Voight, S., Mulch, A., Frish, K., Bartenstein, A., Pross, J., Geres, A., Voigt, T., 2018. Late Oligocene to Early Miocene humidity change recorded in terrestrial sequences in the Ili basin (south-eastern Kazakhstan, Central Asia). Sedimentology 65, 517–539.

Horn, B.L.D., Goldberg, K., Schultz, C.L., 2018. Interpretation of massive sandstone in ephemeral fluvial settings: a case study from the Upper Candelária Sequence (Upper Triassic, Paraná Basin, Brazil). Journal of South American Earth Sciences 81, 108–121.

Hornung, J., Aigner, T., 1999. Reservoir and aquifer characterisation of fluvial architectural elements, Stubensandstein, Upper Triassic, Southwest Germany. Sedimentary Geology 25, 215–280.

Hornung, J., Aigner, T., 2002a. Reservoir architecture in a terminal alluvial plan: an outcrop analogue study (Upper Triassic, Southern Germany), part I: sedimentology and petrophysics. Journal of Petroleum Geology 25, 3–30.

Hornung, J., Aigner, T., 2002b. Reservoir architecture in a terminal alluvial plan: an outcrop analogue study (Upper Triassic, Southern Germany), part II: cyclicity, controls and models. Journal of Petroleum Geology 25, 151–178.

Hounslow, M.W., Ruffell, A., 2006. Triassic: seasonal rivers, deserts and saline lakes. In: Brenchley, P.J., Rawson, P.F. (Eds.), The Geology of England and Wales. The Geological Society London, pp. 295–324.

Huerta, P., Armenteros, I., Silva, P.G., 2011. Large-scale architecture in non-marine basins: the response to the interplay between accommodation space and sediment supply. Sedimentology 58, 1716–1736.

Ielpi, A., Ghinassi, M., 2014. Planform architecture, stratigraphic signature and morphodynamics of an exhumed Jurassic meander plain (Scalby Formation, Yorkshire, UK). Sedimentology 61, 1923–1960.

Ielpi, A., Ghinassi, M., 2015. Planview style and palaeodrainage of Torridonian channel belts: Applecross Formation, Stoer Peninsula, Scotland. Sedimentary Geology 325, 1–16.

Konieczna, N., Belka, Z., Dopieralska, J., 2015. Nd and Sr isotopic evidence for provenance of clastic material of the Upper Triassic rocks of Silesia, Poland. Annales. Societatis Geologorum Poloniae 85, 675–684.

Konietzko-Meier, D., Klein, N., 2013. Growth pattern of *Metoposaurus diagnosticus krasiejowensis* (Amphibia, Temnospondyli) from the Late Triassic of Krasiejów, Poland, as deduced from femur histology. Palaeogeography, Palaeoclimatology, Palaeoecology 370, 145–157.

Konietzko-Meier, D., Sander, P.M., 2013. Long bone histology of *Metoposaurus diagnosticus* (Temnospondyli) from the Late Triassic of Krasiejów (Poland) and its paleobiological implications. Journal of Vertebrate Palaeontology 35, 1–16.

Konietzko-Meier, D., Gruntmejer, K., Marcé-Nogué, J., Bodzioch, A., Fortuny, J., 2018. Merging cranial histology and 3D-computational biomechanics: a review of the feeding ecology of a Late Triassic temnospondyl amphibian. PeerJ 6, e4426. https://doi.org/10.7717/peerj.4426.

Kozur, H.W., Bachmann, G.H., 2010. The Middle Carnian Wet Intermezzo of the Stuttgart Formation (Schilfsandstein), Germanic Basin. Palaeogeography, Palaeoclimatology, Palaeoecology 290, 107–119.

Kraus, M., 1999. Paleosols in clastic sedimentary rocks: their geologic applications. Earth-Science Reviews 47, 41–70.

Kubik, R., Uhl, D., Marynowski, L., 2015. Evidence of wildfires during deposition of the Upper Silesian Keuper succession, southern Poland. Annales. Societatis Geologorum Poloniae 85, 685–696.

Kutzbach, J., Gallimore, R., 1989. Pangaean climates: megamonsoons of the megacontinent. Journal of Geophysical Research-Atmospheres 94, 3341–3357.

Kutzbach, J.E., 1994. Idealized Pangean climates: Sensitivity to orbital change. In: Klein, G. D. (Ed.), Pangea: Paleoclimate, Tectonics, and Sedimentation During Accretion, Zenith, and Breakup of a Supercontinent. Geological Society of America Special Papers 288, pp. 41–55.

Licht, A., Cojan, I., Caner, L., Soe, A.N., Jaeger, J., France-Lanord, C., Mountney, N., 2014. Role of permeability barriers in alluvial hydromorphic palaeosols: the Eocene Pondaung Formation, Myanmar. Sedimentology 61, 362–382.

López-Gómez, J., Arche, A., Pérez-López, A., 2002. Permian and Triassic. In: Gibbons, W., Moreno, T. (Eds.), The Geology of Spain. Geological Society, London, pp. 185–212.

Lucas, S.G., 2015. Age and correlation of Late Triassic tetrapods from southern Poland. Annales. Societatis Geologorum Poloniae 85, 627–635.

Mack, G.H., Madoff, R.D., 2005. A test of models of fluvial architecture and palaeosol development: camp rice formation (upper Pliocene–lower Pleistocene), southern Rio Grande rift, USA. Sedimentology 52, 191–211.

Makaske, B., 2001. Anastomosing rivers: a review of their classification, origin and sedimentary products. Earth-Science Reviews 53, 149–196.

Marynowski, L., Simoneit, B.R.T., 2009. Widespread Late Triassic to Early Jurassic wildfire records from Poland: evidence from charcoal and pyrolytic polycyclic aromatic hydrocarbons. PALAIOS 24, 785–798.

McKie, T., 2014. Climatic and tectonic controls on Triassic dryland terminal fluvial system architecture, central North Sea. In: Martinius, A.W., Ravnås, R., Howell, J.A., Steel, R.J., Wonham, J.P. (Eds.), From Depositional Systems to Sedimentary Successions on the Norwegian Continental Margin. International Association of Sedimentologists Special Publications 46, pp. 19–58.
McKie, T., Williams, B., 2009. Triassic palaeogeography and fluvial dispersal across the northwest European Basin. Geological Journal 44, 711–741.
Miall, A.D., 1996. The Geology of Fluvial Deposits. Sedimentary Facies, Basin Analysis, and Petroleum Geology. Springer-Verlag, Berlin Heidelberg (582 pp.).
Morawska, A., 1997. The Lubliniec fracture zone: boundary of the Upper Silesian and Małopolska massifs, southern Poland. Annales. Societatis Geologorum Poloniae 67, 429–437.
Mücke, A., 1994. Postdiagenetic ferruginization of sedimentary rocks (sandstones, oolitic ironstones, kaolins, and bauxites). Including a comparative study of the reddening of red beds. In: Wolf, K.H., Chilingarian, G.V. (Eds.), Diagenesis, IV, Developments in Sedimentology 51, pp. 361–395.
Nanson, G.C., Rust, B.R., Taylor, G., 1986. Coexistent mud braids and anastomosing channels in an arid zone river: Cooper Creek, Central Australia. Geology 14, 175–178.
Nawrocki, J., Jewuła, K., Stachowska, A., Szulc, J., 2015. Magnetic polarity of Upper Triassic sediments of the Germanic Basin in Poland. Annales. Societatis Geologorum Poloniae 85, 663–674.
Niedźwiedzki, G., Sulej, T., 2008. Lipie Śląskie koło Lisowic – okno na późnotriasowy ekosystem lądowy (Lipie Śląskie of Lisowice – a window on the Late Triassic continental ecosystem). Przegląd Geologiczny 56, 821–822 (In Polish, with English abstract).
Nitsch, E., 2018. The Keuper Group in the Stratigraphic Table of Germany 2016: a continuous or discontinuous stratigraphic record? Zeitschrift der Deutschen Gesellschaft für Geowissenschaften -German Journal of Geology 169, 181–201.
Nordt, L.C., Driese, S.D., 2010. New weathering index improves paleorainfall estimates from Vertisolss. Geology 38, 407–410.
North, C.P., Davidson, S.K., 2012. Unconfined alluvial flow processes: recognition and interpretation of their deposits, and the significance for palaeogeographic reconstruction. Earth-Science Reviews 111, 199–223.
Onoue, T., Yamashita, K., Fukuda, C., Soda, K., Tomimatsu, Y., Abate, B., Rigo, M., 2018. Sr isotope variations in the Upper Triassic succession at Pizzo Mondello, Sicily: constraints on the timing of the Cimmerian Orogeny. Palaeogeography, Palaeoclimatology, Palaeoecology 499, 131–137.
Oszczypko, N., Uchman, A., Bubniak, I., 2012. Foreland provenance of thick conglomerates in the early stage of Carpathian Foredeep development: the case of the Sloboda Conglomerate (Lower Miocene), western Ukraine. Geological Quarterly 56, 789–802.
Paul, J., Wemmer, K., Wetzel, F., 2009. Keuper (Late Triassic) sediments in Germany – indicators of rapid uplift of Caledonian rocks in southern Norway. Norwegian Journal of Geology 89, 193–202.
Pieńkowski, G., 1988. Facial analysis of the uppermost Triassic and the Liassic of the Cracow-Wieluń Upland and prospectes for occurrence of clay deposits. Przegląd Geologiczny 36, 449–456 (In Polish, with English summary).
Pieńkowski, G., Niedźwiedzki, G., Brański, P., 2014. Climatic reversals related to the Central Atlantic magmatic province caused the end-Triassic biotic crisis - evidence from continental strata in Poland. In: Keller, G., Kerr, A.C. (Eds.), Volcanism, Impacts, and Mass Extinction: Causes and Effects. Geological Society of America Special Papers 505, pp. 263–286.
Racki, G., Lucas, S.G., 2018. Timing of dicynodont extinction in light of an unusual Late Triassic Polish fauna and Cuvier's approach to extinction. Historical Biology https://doi.org/10.1080/08912963.2018.1499734.
Racki, G., Szulc, J., 2015. The bone-bearing Upper Triassic of Upper Silesia, southern Poland: integrated stratigraphy, facies and events – introductory remarks. Annales. Societatis Geologorum Poloniae 85, 553–555.
Reineck, H., Singh, I.B., 1980. Depositional Sedimentary Environments. Springer-Verlag, New York (549 pp.).
Reinhardt, L., Ricken, W., 2000. The stratigraphic and geochemical record of Playa Cycles: monitoring a Pangaean monsoon-like system (Triassic, Middle Keuper, S. Germany). Palaeogeography, Palaeoclimatology, Palaeoecology 161, 205–227.
Retallack, G.J., 2001. Soils of the Past. An Introduction to Paleopedology. Blackwell Science, Oxford (404 pp.).
Rust, B.R., Nanson, G.C., 1989. Bedload transport of mud as pedogenic aggregates in modern and ancient rivers. Sedimentology 36, 291–306.
Sarkar, S., Chaudhuri, A.K., 1992. Trace fossils in middle to late Triassic fluvial redbeds, Pranhita Godavari valley, south India. Ichnos: An International Journal for Plant and Animal Traces 2, 7–19.
Sellwood, B.W., Valdes, J.P., 2006. Mesozoic climates: general circulation models and the rock record. Sedimentary Geology 190, 269–287.
Sheldon, N.D., Tabor, N.J., 2009. Quantitative paleoenvironmental and palaeoclimatic reconstruction using paleosols. Earth-Science Reviews 95, 1–52.
Sheldon, N.D., Retallack, G.J., Tanaka, S., 2002. Geochemical climofunctions from North American Soils and application to paleosols across the Eocene-Oligocene boundary in Oregon. Journal of Geology 110, 687–696.
Simon, S.S.T., Gibling, M.R., 2017a. Fine-grained meandering systems of the Lower Permian Clear Fork Formation of north-central Texas, USA: lateral and oblique accretion on an arid plain. Sedimentology 64, 714–746.
Simon, S.S.T., Gibling, M.R., 2017b. Pedogenic mud aggregates preserved in a fine-grained meandering channel in the Lower Permian Clear Fork Formation, north-central Texas, U.S.A. Journal of Sedimentary Research 87, 230–252.
Skawiński, T., Ziegler, M., Czepiński, Ł., Szermański, M., Tałanda, M., Surmik, D., Niedźwiedzki, G., 2017. A re-evaluation of the historical dinosaur remains from the Middle-Upper Triassic of Poland. Historical Biology 29, 442–472.
Słowakiewicz, M., 2003. Fluid inclusion data in calcite from the Upper Triassic hot-spring travertines in southern Poland. Journal of Geochemical Exploration 78, 123–126.
Środoń, J., Szulc, J., Anczkiewicz, A., Jewuła, K., Banaś, M., Marynowski, L., 2014. Weathering, sedimentary, and diagenetic controls of mineral and geochemical characteristics of the vertebrate-bearing Silesian Keuper. Clay Minerals 49, 569–594.
Sulej, T., 2002. Species discrimination of the Late Triassic labyrinthodont *Metoposaurus diagnosticus*. Acta Palaeontologica Polonica 47, 535–546.
Sulej, T., Niedźwiedzki, G., Tałanda, M., Dróżdż, D., Hara, E., 2018. A new early Late Triassic non-mammaliaform eucynodont from Poland. Historical Biology https://doi.org/10.1080/08912963.2018.1471477.
Świło, M., Niedźwiedzki, G., Sulej, T., 2014. Mammal-like tooth from the Upper Triassic of Poland. Acta Palaeontologica Polonica 59, 815–820.
Szulc, J., 2000. Middle Triassic evolution of the northern Peri-Tethys area as influenced by early opening of the Tethys Ocean. Annales. Societatis Geologorum Poloniae 70, 1–48.
Szulc, J., 2005. Sedimentary environments of the vertebrate-bearing Norian deposits from Krasiejów, Upper Silesia, Poland. Hallesches Jahrbuch für Geowisschenschaften, Reihe B 19, 161–170.
Szulc, J., Racki, G., 2015. Formacja Grabowa – podstawowa jednostka litostratygraficzna kajpru Górnego Śląska (The Grabowa Formation – the basic lithostratigraphic unit of the Keuper of Silesia). Przegląd Geologiczny 63, 103–113 (In Polish, with English abstract).
Szulc, J., Gradziński, M., Lewandowska, A., Heunisch, C., 2006. The Upper Triassic crenogenic limestones in Upper Silesia (southern Poland) and their paleoenvironmental context. In: Alonso-Zarza, A.M., Tanner, L.H. (Eds.), Paleoenvironmental Record and Applications of Calcretes and Palustrine Carbonates. Geological Society of America Special Paper 416, pp. 133–151.
Szulc, J., Racki, G., Jewuła, K., Środoń, J., 2015a. How many Upper Triassic bone-bearing levels are there in Upper Silesia (southern Poland)? A critical overview of stratigraphy and facies. Annales. Societatis Geologorum Poloniae 85, 587–626.
Szulc, J., Racki, G., Jewuła, K., 2015b. Key aspects of the stratigraphy of the Upper Silesian middle Keuper, southern Poland. Annales. Societatis Geologorum Poloniae 85, 557–586.
Szulc, J., Racki, G., Bodzioch, A., 2017. Comment on "An early Late Triassic long-necked reptile with a bony pectoral shield and gracile appendages" by Jerzy Dzik and Tomasz Sulej. Acta Palaeontologica Polonica 62, 287–288.
Tal, M., Gran, K., Murray, B., Paola, C., Hicks, D.D., 2004. Riparian vegetation as a primary control on channel characteristics in multi-thread rivers. In: Bennett, S.J., Simon, A. (Eds.), Riparian Vegetation and Fluvial Geomorphology. Water Science and Application 8, pp. 43–58.
Tałanda, M., Bajdek, P., Niedźwiedzki, G., Sulej, T., 2017. Upper Triassic freshwater oncoids from Silesia (southern Poland) and their microfossil biota. Neues Jahrbuch für Geologie und Paläontologie Abhandlungen 284, 43–56.
Tanner, L., 2018. Climates of the Late Triassic: perspectives, proxies and problems. In: Tanner, L. (Ed.), The Late Triassic World - Earth in a Time of Transition. Topics in Geobiology. Springer, pp. 59–90.
Tari, G., Poprawa, P., Krzywiec, P., 2012. Silurian lithofacies and paleogeography in Central and Eastern Europe: implications for shale gas exploration. Society of Petroleum Engineers https://doi.org/10.2118/151606-MS.
Unrug, R., Calikowski, A., 1960. Sedimentation and petrology of the Połomia Beds. Rocznik Polskiego Towarzystwa Geologicznego 30, 129–168 (In Polish with English summary).
Varela, A.N., Raigemborn, M.S., Richiano, S., White, T., Poiré, D.G., Lizzoli, S., 2018. Late Cretaceous palaeosols as paleoclimate proxies of high-latitude Southern Hemisphere: Mata Amarilla Formation, Patagonia, Argentina. Sedimentary Geology 363, 83–95.
Vollmer, T., Werner, R., Weber, M., Tougiannidis, N., Röhling, H.G., Hambach, U., 2008. Orbital control on Upper Triassic playa cycles of the Steinmergel-Keuper (Norian): a new concept for ancient playa cycles. Palaeogeography, Palaeoclimatology, Palaeoecology 267, 1–16.
Wang, P.X., Wang, B., Cheng, H., Fasullo, J., Guo, Z.T., Kiefer, T., Liu, Z.Y., 2014. The global monsoon across timescales: coherent variability of regional monsoons. Climates of the Past 10, 2007–2052.
Williams, G.P., 1986. River meanders and channel size. Journal of Hydrology 88, 147–164.
Zamanian, K., Pustovoytov, K., Kuzyakov, Y., 2016. Pedogenic carbonates: forms and formation processes. Earth-Science Reviews 157, 1–17.
Zatoń, M., Piechota, A., Sienkiewicz, E., 2005. Late Triassic charophytes around the bone-bearing bed at Krasiejów (SW Poland) – palaeoecological and environmental remarks. Acta Geologica Polonica 55, 283–293.
Zatoń, M., Niedźwiedzki, G., Marynowski, L., Benzerara, K., Pott, C., Cosmidis, J., Krzykawski, T., Filipiak, P., 2015. Coprolites of Late Triassic carnivorous vertebrates from Poland: an integrative approach. Palaeogeography, Palaeoclimatology, Palaeoecology 430, 21–46.